



**MULTI-DIMENSIONAL SEISMIC INVERSION**

by

**Jack K. Cohen and Norman Bleistein**

**Partially supported by the Selected Research  
Opportunities Program of the Office of Naval Research.**

**Prepared for a short course**

**ASYMPTOTIC METHODS FOR SEISMIC MODELING AND INVERSION**

**presented at**

**The University of Trondheim  
Trondheim, Norway  
October 6-17, 1986**

**Center for Wave Phenomena  
Department of Mathematics  
Colorado School of Mines  
Golden, Colorado 80401  
Phone: (303) 273-3557**



## Preface

These notes were prepared to be used in conjunction with the textbook, *Mathematical Methods for Wave Phenomena*, Bleistein (1984), in a two week short course to be presented at the University of Trondheim, October 6-17, 1986. The format will be half day lectures based on these notes and current papers and half day lectures based on the textbook. In this manner, we plan to cover both the necessary mathematical tools and their use in direct modeling and inversion.

Material from Chapters 1, 2, 8, and 9 of the textbook will be covered. Thus, these notes either omit entirely or contain only brief discussions of the following topics: the method of stationary phase in one and higher dimensions; the ray method (geometrical optics and geometrical theory of diffraction), the eikonal equation and the transport equation; the Kirchhoff approximation; the singular function of a surface and mathematical imaging.



## TABLE OF CONTENTS

1. Introduction.....	1.1
2. The Born Integral Equation.....	2.1
2.1 The acoustic assumption.....	2.1
2.2 Perturbation assumption.....	2.4
2.3 The Born approximation.....	2.6
2.3.1 Born approximation and high frequency.....	2.6
2.3.2 Implementation of the Born approximation.....	2.9
2.4 Special cases.....	2.11
2.5 Summary.....	2.15
3. Theoretical and Physical Constraints.....	3.1
3.1 The high frequency assumption.....	3.1
3.1.1 Edge sharpening.....	3.3
3.1.2 Extraction of information from bandlimited delta functions.....	3.6
3.2 Effect of linearization.....	3.15
3.3 Processing field data.....	3.19
3.4 The effects of finite aperture and discretization.....	3.20
3.5 Summary.....	3.25
4. Zero-offset Constant Reference Inversion.....	4.1
4.1 Three dimensional algorithm.....	4.2
4.2 High frequency approximations.....	4.11
4.3 Two-and-one-half dimensional limit.....	4.16
4.4 Verification for model data.....	4.19
4.4.1 Verification for a horizontal plane.....	4.20
4.4.2 Kirchhoff scattering data.....	4.23
4.4.3 Verification for a general single surface.....	4.25
4.5 Implementation and examples.....	4.43
4.6 Summary.....	4.45
5. Towards a High Frequency Inversion Formalism.....	5.1
5.1 Deducing the inversion kernel from Kirchhoff data.....	5.2
5.2 Deducing the inversion kernel by the asymptotic completeness principle.....	5.5
5.3 Toward a generalization of the completeness relation approach.....	5.11
5.4 Test case: inclusion of field statics.....	5.14
5.5 Generalizations.....	5.18
5.6 Summary.....	5.18
Bibliography.....	B1



## 1. Introduction

For more than a decade, we have been engaged in research on inverse methods with application primarily to imaging the interior of the earth on length scales of interest in seismic exploration and seabed mapping. The methods we use are classical employing partial differential and integral equations, perturbation techniques, integral transforms, and asymptotic and numerical analysis to arrive at computer algorithms which produce a reflector map of the interior of the earth and also provide a means of estimating the change in medium parameters across the reflectors.

### Inverse Problems

The mapping of the interior of the earth from observations on the surface of the earth, or in the ocean, is an inverse problem. For this type of inverse problem, the propagation of signals -- acoustic, elastic or electromagnetic -- into the earth is modeled by the appropriate equation or system of equations in which functions characterizing the interior (acoustic, elastic, or electromagnetic parameters) are left free. One or more signals consistent with the model are introduced at or near the surface of the earth in a region of interest. The "irregularities" of the interior of the earth produce a response to those signals. Observations of those responses are recorded. The objective of inverse methods is to determine the free coefficients in the modeling equations from knowledge of the input signal(s) and the response(s) and thereby "map" the interior. This type of problem is known as an inverse scattering problem. This contrasts with the more familiar direct scattering problem in which the parameters in the

equation(s) are known and the objective is to determine the response to a given source in some domain of interest.

### Migration and Inversion

At one time, we thought of migration as a process whereby a reflector map is produced, with little concern or emphasis on parameter estimation. In that sense, migration is a partial inversion, namely, an inversion for structure alone. At the present time, the demarcation between migration and inversion is fuzzier, with the objectives of modern migration techniques being almost identical with those of inversion. Indeed, migration and inversion algorithms themselves are almost identical when they start from the same earth model and have the same objectives as regards reflector mapping and parameter estimation. The real difference would seem to be in approach and philosophy; migrators think primarily in terms of back projecting or downward propagating the ensemble of surface observations, while inverters think of "solving" some governing equation(s) for the unknown earth parameters. Then, migrators see reflectors as "events" in the back projected waves, while inverters see reflectors as discontinuity surfaces of the solutions of their governing equations. We believe that the researcher who understands both is better off, no matter which he/she favors for their own research and/or implementation. As mathematicians we tend to emphasize explicit statements of assumptions. This sometimes causes alarm - - but, afterall, the restrictions are the same whether one states or not!

### The Earth as a Fluid

Until quite recently, our research was concentrated on modeling the earth as a constant density fluid in which the objective was to determine an acoustic reflector map and estimate only the change in sound speed across the reflectors. On the one hand, this is an extremely primitive model of wave propagation in the earth. On the other hand, this primitive model has a long history in seismic exploration, both in direct scattering and inverse scattering or migration.

There is good reason for this. First, in cases in which the source and receiver are relatively close together and a compressional source is used, the observed response is dominated by the compressional wave, which is well modeled by acoustic wave propagation for the frequencies and length scales of interest in seismic exploration. Hence, there is useful information about the earth's interior in the inversion of seismic data in accordance with the acoustic model. Second, when the range over which waves propagate is sufficiently large (almost always true in seismic exploration) the compressional and shear modes propagating to the surface are well separated. From the point of view of arrival times of signals, the acoustic wave equation provides a good model of the propagation of shear waves. (That is, the phase fronts or wave crests propagate according to the same equation for either type of wave, with only the propagation speed differing in the two problems.) Third, there are the practical problems of gathering and processing three component data for full elastic wave equation inversion. Fourth, there is much to be learned about the harder elastic inverse problem from the simpler acoustic inverse problem. There are degrees of complexity of the inverse problem for which the harder elastic problem has a direct analog in the simpler acoustic problem (e.g., source/receiver configuration and a priori "knowledge" about the earth parameters). We treat these

complexities in a hierarchical manner, from simpler to harder. We can best explain our philosophy about long term concern with addressing this hierarchy for the acoustic model via the rhetorical question, "If you can't solve the easier (acoustic) problem, why are you trying to solve the harder (elastic) problem?" Indeed, it is only quite recently that we have felt ready to apply our methods to the two parameter acoustic model and the elastic model. Research on both of these models is now in progress in our group.

### The Nonlinearity of the Inverse Problem

The inverse problem is nonlinear. The wave propagation model contains products of the unknown field in the interior of the earth with the unknown earth parameters. In almost all approaches to solution of the inverse problem, linearization is achieved by introducing reference values of the earth parameters and, in some sense, "back projecting" or "back propagating" the observed data into the earth with respect to these background values.

One branch of the hierarchy mentioned above is characterized by the increasing complexity of the background parameters, from constant, to dependence on one spatial variable, then two, then three. One can think of the background as a zeroth order estimate of the earth parameters and the output of the inversion as a correction to this estimate. One might then contemplate correcting the background and re-solving the inverse problem with this new background in an iterative or recursive manner.

### Source/Receiver Configurations

The complexity of the source/receiver configuration provides another branch of the hierarchy of inverse problems we consider. There are two ways of viewing the configurations. First, there are the experiments as they are performed in the field. Second, there are the model configurations, which are designed to more closely model reality with increasing complexity. In practice, data is generated via an ensemble of common (or single) source experiments in which the data is observed at a finite array of receivers. The data can be re-ordered as common receiver data, common midpoint data or common offset data, etc.

Conceptually, the simplest model experiment is a single common source experiment with receivers "everywhere" on the surface. The observed signal may be back projected into the earth with respect to the background propagation speed and reflectors are determined as events where the back projections of the observations coincide with the downward propagation from the source.

In practice, the receiver array is not broad enough to allow for inversion from a single experiment alone. Hence, one must consider an ensemble of experiments.

The simplest case of an ensemble to consider is the set of zero-offset or backscatter experiments. This model is not achieved in the field. (Again, if you can't handle this problem ... .) However, data which approximates zero-offset data is obtained by application of various pre-processing techniques ("stacking").

In migration, it is assumed that such an ensemble of observations constitutes boundary values for a wave whose propagation is governed by the same wave equation, again with halved background propagation speed. There is overwhelming evidence of the validity of this assumption. It is also a

conclusion of the inversion approach to reflector mapping.

Much of our inversion research has addressed this zero-offset configuration with increasing complexity of background propagation speed. With only data from this experiment, one maps reflectors as impedance discontinuities. If constant density is also assumed, then the inversion provides a means for estimating the jump in propagation speed, as well.

A common offset data set leads to a more difficult inverse problem, but a single offset still leads to the estimation of a single parameter as above. Given data sets for two offsets, it is possible to invert for two parameters, sound speed and density, with the stability of the two estimates still a subject of research. In practice, one could use more offsets to improve the stability and accuracy of the estimates.

As previously mentioned, field data is actually an ensemble of common source experiments, with a finite aperture of receivers recording data for each source. Each common offset data set of the previous inverse problem is extracted by reordering the data of this ensemble of experiments. Since the ensemble of common source experiments contains many common offset data sets, the same type of inversion is possible for this model as for the previous one.

### Two-and-one-half Dimensions

Most seismic data sets are gathered over a line on the surface of the earth, rather than over an areal or surface array. In such a case, one cannot hope to invert for three dimensional variations in the earth parameters. Thus, we must create a model and establish an inverse problem with goals that are consistent with the data as gathered. We assume that

the parameters we seek vary only in two dimensions, namely, depth and along the line of observations, with no variations in the orthogonal transverse direction. However, we can nonetheless allow three dimensional propagation of the waves in the earth. We refer to this model in which we allow for three dimensional propagation over an earth with two dimensional variation as two-and-one-half dimensional or 2.5D.

### The Theory

For the acoustic model, we will develop the theory for reflector mapping and estimation of sound speed and density variations across reflectors in 2.5D and 3D, with background parameters varying in complexity from constant to dependence on three spatial variables, for zero-offset, more general common offset, or common source or common receiver experiments.

### Computer Implementation

The structure of computer codes to implement our theories all follow the same basic pattern, with modules of the overall code requiring modification to account for increasing complexity of the model. These will be discussed in context.

## 2. The Born Integral Equation

In this chapter we will derive a general integral equation for the fluctuations in acoustic impedance. The result is equation (2.15), the "Born integral equation." We will also discuss the meaning and validity of the assumptions required for the derivation. The principle ones are:

- (1) The fields are adequately described by the scalar wave equation.
- (2) The sources are adequately described by 3-D point sources.
- (3) The velocity (or impedance) is adequately described by a known reference function plus "small" perturbations.

### 2.1. The acoustic assumption and the point source model

We will make the acoustic approximation. That is, we assume that the fields are governed by the scalar wave equation. Although we are beginning to see attempts to honor the elastic wave equation (e.g., Kuo and Dai, 1984, Boyse and Keller, 1986), most of the current migration and inversion literature still makes this assumption.

To make things simpler, we will also assume a constant density model of the earth. In fact, if we retain density, then we would not have to modify our discussions of the location of reflectors, but we would have to modify the amplitude of our inversion operators and we would have to replace "reflection coefficient" by "impedance coefficient" throughout. It is pedagogically simpler to discuss the constant density case first and to introduce the question of density variations much later in the development.

We model our sources as 3-D point sources -- Dirac delta functions. We

remark that the plane wave source was treated for a variety of cases in Cohen and Bleistein (1977). Generally speaking, the plane wave source is easier to treat. We adopt the point source model because it is closer to the geophysical exploration reality -- although, it too, is an idealization of the real world. With these two assumptions, we can state our governing equation as

$$\left[ \nabla^2 - \frac{1}{v^2(\underline{x})} \frac{\partial^2}{\partial t^2} \right] U(t, \underline{x}, \underline{x}_s) = - \delta(t) \delta(\underline{x} - \underline{x}_s) \quad (2.1)$$

Here,

$$\underline{x} = (x, y, z), \quad \underline{x}_s = (x_s, y_s, z_s), \quad (2.2)$$

where  $\underline{x}$  denotes the field point,  $\underline{x}_s$  denotes a generic "source" point, and

$$\nabla^2 = \frac{\partial^2}{\partial x^2} + \frac{\partial^2}{\partial y^2} + \frac{\partial^2}{\partial z^2} \quad (2.3)$$

Note that we nominally start the source at a nominal time,  $t = 0$ . That is, we normalize each source to zero time, even though, in the field, each experiment is carried out at a different time. This normalization relies on the "time invariance" of the geophysical system on the exploration time scale.

Usually we think of  $U$  as measuring the compressive wave. However, the above equation applies equally well to certain shear source surveys where the uncoupled shear mode is observed. On the other hand, it does not apply to the mode-converted PSSP waves sometimes observed at wide angle; to treat

this phenomenon, we must base our derivation on the elastic wave equation.

It is usually more convenient to work in frequency domain, so we apply the temporal Fourier transform operator,

$$f(\omega) = \int_0^{\infty} dt e^{i\omega t} F(t) , \quad (2.4)$$

$$u(\omega, \cdot, \cdot) = \int_0^{\infty} U(t, \cdot, \cdot) e^{i\omega t} dt .$$

to obtain the Helmholtz equation:

$$\left[ \nabla^2 + (\omega/c)^2 \right] u(\omega, \underline{x}, \underline{x}_s) = - \delta(\underline{x} - \underline{x}_s) . \quad (2.5)$$

We remark that implicit in our definition of the Fourier transform, (2.4), is the assumption that we are dealing with "causal" functions, that is functions that are zero up to time zero (more generally, up to some finite time). This assumption implies certain properties in  $\omega$  of the functions we are considering. In particular, all of our functions are analytic for complex  $\omega$  in the upper half plane,  $\text{Im } \omega > 0$ . Furthermore, all of these functions must approach zero as  $|\omega| \rightarrow \infty$  in that domain. This observation provides a basis for picking certain complex valued functions of  $\omega$  which appear later in the development. That is, any solution to the wave equation that we consider cannot become unbounded for  $\omega$  in the upper half plane.

## 2.2. Perturbation assumption

We assume that the unknown sound speed,  $v$ , can be accurately represented by a known reference sound speed,  $c$ , plus a "small" relative perturbation,  $a$ :

$$\frac{1}{v^2(\underline{x})} = \frac{1}{c^2(\underline{x})} \left[ 1 + a(\underline{x}) \right]. \quad (2.6)$$

Define an "incident" acoustic field, that satisfies the equation with the known reference sound speed:

$$\left[ \nabla^2 + (\omega/c)^2 \right] g(\omega, \underline{x}, \underline{x}_s) = - \delta(\underline{x} - \underline{x}_s) \quad (2.7)$$

We use the notation "g" because our incident field is so patently a "Green's function." Indeed, given the equation,

$$\left[ \nabla^2 + (\omega/c)^2 \right] h(\omega, \underline{x}) = - f(\underline{x}), \quad (2.8)$$

with arbitrary source function, "f", we have at once the "zero-state" solution for "h":

$$h(\omega, \underline{x}) = \iiint d^3 \underline{x}' g(\omega, \underline{x}', \underline{x}) f(\underline{x}') \cdot \quad (2.9)$$

The representation of  $g$  (discussed later) simplifies somewhat when the background speed,  $c$ , is assumed continuous, and so we make this assumption as well. The discontinuous case is discussed in Cohen and Bleistein (1977),

Lahlou et al. (1983) and Bleistein et al. (1985).

We introduce the "scattered" field,  $u_S$  as

$$u_S(\omega, \underline{x}, \underline{x}_S) = u(\omega, \underline{x}, \underline{x}_S) - g(\omega, \underline{x}, \underline{x}_S) \quad (2.10)$$

and find that (2.1), (2.6) and (2.10) imply

$$\left[ \nabla^2 + (\omega/c)^2 \right] u_S(\omega, \underline{x}, \underline{x}_S) = - \omega^2 \frac{\alpha(\underline{x})}{c^2(\underline{x})} u(\omega, \underline{x}, \underline{x}_S) . \quad (2.11)$$

Exercise 2.1. Establish this result.

Denoting a generic geophone (i.e., receiver) by  $\underline{x}_g$ , we identify

$$u_S(\omega, \underline{x}, \underline{x}_S) \Big|_{\underline{x} = \underline{x}_g} = u_S(\omega, \underline{x}_g, \underline{x}_S) \quad (2.12)$$

with the field observed at the geophones. This identification is another facet of the perturbation assumption. Indeed, its accuracy depends on the Green's function,  $g$ , being a good approximation to the actual incident field. In turn this approximation is accurate only if the reference velocity,  $c$ , is close to the actual velocity,  $v$ , which is just the perturbation assumption.

Since (2.11) is a special case of (2.8), we can apply (2.9) to obtain

$$u_S(\omega, \underline{x}', \underline{x}_S) = \omega^2 \iiint d^3 \underline{x} g(\omega, \underline{x}', \underline{x}) \frac{\alpha(\underline{x})}{c^2(\underline{x})} u(\omega, \underline{x}, \underline{x}_S) . \quad (2.13)$$

In applying (2.9),  $\underline{x}_S$  is just a parameter that "comes along for the ride."

That is, (2.9) is applied for each value of this parameter.

### 2.3. The Born approximation

Since  $\alpha$  is "small", and since  $u_g$  has a source term proportional to  $\alpha$ , it is reasonable to think that  $u_g$  is small (of order  $\alpha$ ). If we accept this, then on splitting up  $u$  in the source term into its constituents,

$$\alpha u = \alpha(g + u_g), \quad (2.14)$$

we see that the second term is of second order in  $\alpha$  and hence is small compared to the first term.

The neglect of this term,  $\alpha u_g$ , compared to the first term,  $\alpha g$ , is known as the "Born approximation". Obviously, its validity is still another aspect of the perturbation assumption. However, one cannot rigorously derive it from that assumption, because it isn't always true! Think, for example, of wide angle high amplitude refraction arrivals. Nonetheless, if the perturbation assumption is accurate then most of the observed signal consists of weak reflections and the Born approximation is justified (see the next section and Exercise 2.4 below).

#### 2.3.1. Born approximation and high frequency

It might appear that the Born approximation requires low frequency because of the  $\omega$  squared multiplier on the right side of (2.11). That is not quite the case. Indeed, in that equation, we see that the right side contains a product in which the frequency and  $\alpha$  are "competing" to determine the ultimate magnitude of the source for  $u_g$ . However, the situation is far

from hopeless.

First, let us suppose that the reference sound speed,  $c(\underline{x})$ , were exact, down to some reflector. In that case,  $\alpha(\underline{x}) \equiv 0$  down to that reflector. It will become apparent as we proceed that proper location of reflectors depends directly on proper estimation of the propagation speed down to the reflector. Thus, in this case, we would expect that the location of the first reflector would be perfect -- independent of the jump in  $\alpha$  at that reflector -- and any errors in the inversion down to this reflector could only occur in linearized estimates of reflection strength at that reflector. As we will see below, it is possible to compensate for these.

Furthermore, high frequency solutions of the wave equation tend to have the form  $u = A \exp\{i\omega\tau\}$ , with  $A$  being an inverse series in  $i\omega$  with each coefficient in the series and  $\tau$ , as well, depending only on the spatial variables. An overall multiplier of a power of  $\omega$  is possible, as well.

Let us consider substituting such a form into (2.11) for  $u_g$  and  $g$ . Then, except for that overall power, the leading order in  $\omega$  on both sides of (2.11) is  $O(\omega^2)$ . The Laplacian contributes such a term with coefficient  $-(\nabla\tau)^2 u_g$ . We find, then, that the multiplier,  $\omega^2$ , divides out of this leading order term, leading to the conclusion that  $u_g = O(\alpha)$  at high frequency, independent of  $\omega$ .

Unfortunately, this analysis does not prevail throughout the spatial domain, but only in a restricted region. However, that region is just where seismic data is collected!

As an example of a region where this analysis does not apply, consider the forward scattering or downward propagating direction. In that direction, the wave denoted by  $g$  and defined by (2.7) accumulates a phase error relative to the "true" downward propagating wave, that error being

approximately  $i\omega/a/c^2 ds$ , where  $s$  denotes arclength along the geometrical optics rays or paths of propagation. With increasing propagation through the region of nonzero  $\alpha$ , this integral will increase in magnitude, eventually attaining the value  $\pi$ . At such places,  $g$  and the true downward field are of opposite sign and the field we call  $u_g$  will have to undo this error, which is order unity in  $\alpha$ . Consequently, the downward propagating part of  $u_g$  cannot be only  $O(\alpha)$ .

On the other hand, at high frequency, the upward propagating part of  $u_g$  arises from reflections at jump discontinuities of  $\alpha$ . At normal incidence, such waves are scaled by a reflection coefficient proportional to the jump in  $\alpha$ , hence, certainly  $O(\alpha)$ . For small offset angles between incidence and reflection, this remains the case, but as the offset angle increases towards critical, the reflection coefficient approaches one. For small jumps in  $\alpha$ , that critical angle will be large; for larger jumps in  $\alpha$ , that critical angle decreases.

Now we have some idea where we can expect that the upward scattered field will be  $O(\alpha)$ . The offset angle between incidence and reflection should be relatively small compared to the critical angle. For the common source, common receiver and common offset experiments considered here, this is the case.

Later we will show that the inversions based on the Born approximation for the upward scattered data actually have an even broader range of validity than their basis in the Born approximation gives us a right to expect. The way we will do this is to apply the inversion formulas to Kirchhoff approximate data for a single reflector.

The Kirchhoff approximation has the feature that it is not constrained to small increments in sound speed across the reflector, nor to angles which

are small compared to the critical angle. We will find that applying the inversion operator to such data produces an output from which we can measure the increment in sound speed without linearization, that is, without the constraint that the increment be small.

Thus, to a degree, we shall have removed the small perturbation constraint of the Born approximation. To properly locate the "test reflector," it will still be necessary that the background or reference speed above the reflector be "close" in some sense to the true value. It will also be necessary that multiples from reflectors above the test reflector be small enough that they can be disregarded. In this sense, we shall not have completely dispensed with the smallness of  $\alpha$ . However, this type of result anticipates a recursive application of these methods in which one uses information gained at each reflector to progressively improve the estimate of the background speed further into the subsurface, thereby properly locating the next reflector and estimating its reflection strength.

In summary, then, the Born approximation is a vehicle for getting started. Its use in conjunction with high frequency is acceptable for the seismic experiments under consideration. Extension of the basis of validity of our inversion schemes will provide a means to overcome many of the constraints of the original derivation.

### 2.3.2. Implementation of the Born approximation

We now make the Born approximation -- i.e., neglect the term  $\alpha_{\text{g}}$  in (2.14) and evaluate  $u_{\text{g}}$  (2.13) on the observation datum to obtain the Born integral equation,

$$u_S(\omega, \underline{x}_g, \underline{x}_s) = \omega^2 \iiint d^3 \underline{x} \frac{g(\omega, \underline{x}_g, \underline{x}) g(\omega, \underline{x}, \underline{x}_s)}{c^2(\underline{x})} \alpha(\underline{x}) . \quad (2.15)$$

Appealing to the symmetry property of Green's functions, we obtain the alternate form:

$$u_S(\omega, \underline{x}_g, \underline{x}_s) = \omega^2 \iiint d^3 \underline{x} \frac{g(\omega, \underline{x}, \underline{x}_g) g(\omega, \underline{x}, \underline{x}_s)}{c^2(\underline{x})} \alpha(\underline{x}) \quad (2.16)$$

for the unknown velocity perturbation  $\alpha$ . We remark that we do not have the same symmetry for the variable density case and must use (2.15), instead, or make the appropriate adjustment in (2.16).

Exercise 2.2. Show that the Green's function has the indicated symmetry property which leads to (2.16).

Exercise 2.3. Give an alternate derivation of the Born inversion integral equation based on applying Green's theorem to  $g$  and  $u_S$ .

Exercise 2.4. Discuss the common practice of "muting" the early refraction arrivals before applying a standard migration algorithm. Is the perturbation assumption also required to justify the migration procedure? (See, e.g., Schultz and Sherwood, 1980; Bleistein and Cohen, 1979; Claerbout, 1976, 1985.)

We have carried out the derivation of the Born integral equation as if the medium was free space. However, we can adapt the derivation to the half

space model, which is more appropriate to geophysics, by imposing the condition that  $\alpha$  vanish "above" the geophones,  $\underline{x}_g$ . It is also possible to repeat the derivation using a half space model from the start. In this case, one uses a homogeneous wave equation, excited by boundary impulsive sources. If the boundary source is defined appropriately, the same integral equation is obtained.

#### 2.4. Special cases

We consider two types of specializations:

- (1) Spatial Dependence of Reference Velocity;
- (2) Source/Receiver Configurations.

The spatial dependence can be:

$$\text{Constant reference speed, } c = \text{Constant}; \quad (2.17)$$

$$\text{Stratified reference speed, } c = c(z) \quad (2.18)$$

$$\text{Laterally varying reference speed, } c = c(x,z) \quad (2.19)$$

$$\text{General 3-D reference speed, } c = c(x,y,z) . \quad (2.20)$$

Recall that we have imposed a continuity constraint on the reference speed. This constraint is not essential, but it allows us to dispense with the bookkeeping involved in maintaining and propagating the family of reflection/transmission coefficients that would otherwise develop at built-in discontinuities. Also, we rarely have sufficient confidence in our a priori knowledge to want to build in abrupt changes at precise locations.

Usually a "ramp" transition function more accurately represents the state of our knowledge (or ignorance) about the subsurface across the region of change.

Our basic theory encompasses curved observation surfaces. However, for the present we consider some special cases in which the sources and receivers are located on the flat datum  $z = 0$ . Consistent with the remarks above, we shall then assume that

$$\alpha(\underline{x}) = 0, \quad z < 0. \quad (2.21)$$

If we then denote the location of a point on  $z = 0$  by the two-vector,

$$\underline{\xi} = (\xi, \eta), \quad (2.22)$$

we can succinctly characterize the most important source-receiver configurations as follows:

Common source gather,

$$\underline{x}_s = (\underline{\xi}_0, 0) \quad , \quad \underline{x}_g = (\underline{\xi}, 0) \quad , \quad \underline{\xi}_0 \text{ fixed}, \quad (2.23)$$

Common receiver gather,

$$\underline{x}_s = (\underline{\xi}, 0) \quad , \quad \underline{x}_g = (\underline{\xi}_0, 0) \quad , \quad \underline{\xi}_0 \text{ fixed}, \quad (2.24)$$

Common midpoint gather,

$$\underline{x}_s = (\underline{m} - \underline{\xi}, 0) \quad , \quad \underline{x}_g = (\underline{m} + \underline{\xi}, 0) \quad , \quad \underline{m} \text{ fixed}, \quad (2.25)$$

Common offset gather,

$$\underline{x}_s = (\underline{\xi} - \underline{h}, 0) \quad , \quad \underline{x}_g = (\underline{\xi} + \underline{h}, 0) \quad , \quad \underline{h} \text{ fixed} \quad . \quad (2.26)$$

Note that only the first of these configurations corresponds to a physical experiment; all the rest are synthetic gathers obtained by rearranging the data. For the first part of this course, we consider a special case of the common offset configuration, the

Zero offset gather:

$$\underline{x}_s = \underline{x}_g = (\underline{\xi}, 0) \quad . \quad (2.27)$$

This configuration is often well approximated by CMP "stacked" data, but there are times when the approximation fails completely. There is a good discussion of this issue in Schneider (1984).

Intuitively, if we are to recover a subsurface image with three degrees of freedom, it seems that our input data set should also have three degrees of freedom. As in the above examples, two of these degrees come from the source/receiver configuration. The remaining degree of freedom must come from something analogous to depth--clearly this is the time dimension! Indeed, we observe for some number of seconds and the depth to which we can reconstruct the subsurface is directly related to the elapsed time over which we can observe useful signals. In our mathematical derivation, we have replaced the physical time dimension by its Fourier equivalent, the

frequency dimension.

In the 3-D problem, the sources can have up to two degrees of freedom-- a set of positions on the observation surface. Similarly, the receiver positions can have up to two degrees of freedom. However, this is more surface data than is required to do an inversion/migration and so we have, in each case, stated two restrictions on the source/receiver positions, leaving a net of two degrees of freedom.

In cases where we have more than the minimal number of degrees of freedom in the source/receiver configuration, we can use the extra data to make our migrations/inversions more robust -- for example, by the use of least squares. We can also use this extra freedom to attempt an estimation of additional parameters. Clayton and Stolt (1981) pursue both of these themes. Coen (1981, 1982), Raz (1981a, 1981b) and Eiges and Raz (1985), Bleistein (1986) pursue multiparameter estimation.

One should not become too enthusiastic about counting degrees of freedom. An appropriate number of degrees of freedom in the data set does not imply that inversion is possible. Such counting arguments merely serve to eliminate some cases in which the data set is clearly inadequate.

Exercise 2.5. Specialize the above source/receiver configurations to the case of observation on a line. In this case, what is a reasonable migration/inversion goal?

Exercise 2.6. What is a reasonable goal for a single source/receiver pair? (Ignore noise or assume that the experiment can be repeated many times.)

Exercise 2.7. Characterize one or more VSP source/receiver configurations -- obviously we have to abandon equation (2.22).

Exercise 2.8. Characterize the common source configuration for a curved observation surface -- again we must abandon (2.22).

Exercise 2.9. Can we use extra degrees of freedom in the source/receiver configuration to replace the time/frequency dimension? (See Coen, 1981, for example.)

## 2.5. Summary

The main result of this chapter is equation (2.15), the Born integral equation. We have derived it for the acoustic wave equation and point sources using the perturbation assumption (2.6) that states that the total velocity field is accurately represented by small fluctuations from a known reference velocity. The Born integral equation has been derived for an arbitrary source/receiver configuration and arbitrary continuous reference velocity. We have pointed out several special cases of interest.

### 3. Theoretical and Physical Constraints

In this chapter, we give some plausibility arguments about what can and cannot be expected from inversions based on the perturbation (Born) approximation. These observations have wide applicability. However, to avoid obscuring the main points, we use simple models as illustrations. In particular, we assume a constant reference velocity in these preliminary discussions.

In this simple context, we will explore the effects of bandlimiting and linearization. We will also give a brief introduction to the effects of finite aperture and discretization in both time and space.

A major conclusion is that the use of high frequency approximations is usually justified. Although our first inversion will be obtained without making this assumption, high frequency approximations are at the heart of recent inversion developments.

#### 3.1. The high frequency assumption

Real seismic data is inevitably bandlimited data. Roughly speaking, the loss of the low end of the spectrum entails degradation of the overall trend of the data, while the loss at the high end implies lowered resolution of reflectors. Although we have losses at both the high and low ends of the frequency spectrum, it happens that in most interpretable seismic data, the data resides in the high frequency portion of the spectrum. This may seem a dubious assertion in light of the fact that a typical seismic data set has a three octave spectrum from 6 Hz. to 48 Hz. Such numbers may not seem large in an absolute sense. However, we could certainly have expressed them as

6000-48000 milHz! Obviously we require a non-dimensional quantity before rendering a judgement: frequencies adequate to image an elephant will be inadequate for imaging a gnat. It will turn out that the appropriate non-dimensional quantity for migration/inversion is

$$\Lambda = 4\pi fL/c . \quad (3.1)$$

Here  $f$  is conservatively estimated as the lowest frequency used,  $L$  denotes any of the length scales of the problem and  $c$  is a typical propagation speed. In many mathematical and physical problems it turns out a non-dimensional parameter is large enough to justify asymptotic (here "high frequency") approximations when it exceeds 3. That is, parameter values greater than 3 typically incur errors of only a few percent. See Bleistein (1984) for examples and further discussion.

Since our  $\Lambda$  has a factor of  $\pi$ , let us, for argument's sake, take the high frequency regime to be

$$\Lambda > \pi . \quad (3.2)$$

For  $f = 6$  Hz and  $c = 2000$  m/s, this restricts the "typical" length to be greater than 83 m (250 ft). What are some "typical" exploration length scales? Reflector depth is one -- reflector depths of interest are usually much greater than 80 meters. When we need to image shallower reflectors, nature cooperates: much higher frequencies can be recovered for near surface surveys (perhaps as high as 400 Hz). Another length scale is reflector curvature--again these are usually above our minimum.

It is, of course, possible to come up with valid exploration counterexamples -- thin bed resolution being a primary instance. However, it

must be realized that when the high frequency limit is violated, all imaging methods fail, since the very notion of imaging involves the assumption of high frequency. Think, for example, of the use of "rays", "wavefronts" and "reflectivities" (all high frequency notions) in various migration techniques. When the data does not contain the frequencies required for imaging, then no mathematical trickery can save us! On the other hand, we often do have high frequency information adequate to interpret many horizons of interest.

As noted earlier, for the first simple inversion model we shall study, we can obtain a "wide-band" inversion. In particular, we need not assume that the data is high frequency. However, the high frequency assumption allows us to get a computationally more effective algorithm with no degradation of most real -- that is, bandlimited -- data sets. For more complex inversion models, we will use the high frequency assumption ab initio in deriving inversion algorithms.

Once we limit ourselves to trying to obtain only the information available from high frequency data, we can exploit certain features of that type of data to sharpen the images of the reflectors we seek and to estimate the change in sound speed across each reflector. In the next two subsections, we describe these features of processing high frequency data.

### 3.1.1. Edge sharpening

The inversion quantity,  $\alpha$ , ideally consists of Heaviside step functions across the interfaces. However, due to bandlimiting, the ideal sharp edge of the steps will be smeared, making it hard to accurately estimate the

interface locations. The problem of "edge sharpening" occurs in many imaging contexts and is usually handled by taking a spatial derivative of some sort. Furthermore, since derivatives are merely multiplications in (spatial) Fourier domain, the differentiation operation is usually carried out in this domain.

In many geophysical contexts, the assumption of small dip is valid. In such cases, a z-derivative would do a passable job. However, this introduces a cosine of the dip into the output that later has to be "backed out" of the inversion if parameter estimation is desired. Also, large dips may be irrecoverably degraded by having their reflection strength diminished to near or below the noise level.

In image processing, a "Laplacian" filter is often used to do edge sharpening. This operator has the virtue of being isotropic -- it does not favor any particular spatial direction as does the z-derivative. This desirable behavior is counterbalanced by the fact that in interpreting seismic sections, we wish to see sinc-like behavior with peaks at the reflectors. The Laplacian operator is a second derivative and (loosely) would convert the steps of  $\alpha$  into doublets -- we really want a first derivative operator! This leads to the notion of using the square root of the Laplacian operator, which provides a first order isotropic operator. In Fourier domain, the Laplacian operator is given by the correspondence

$$\nabla^2 = \left[ \frac{\partial^2}{\partial x_1^2}, \frac{\partial^2}{\partial x_2^2}, \frac{\partial^2}{\partial x_3^2} \right] \Leftrightarrow -k^2 = - \left[ k_1^2 + k_2^2 + k_3^2 \right] \quad . \quad (3.3)$$

Employing the dispersion equation for the wave equation,

$$\omega = ck \quad , \quad (3.4)$$

we obtain the isotropic first derivative operator in the form  $i\omega/c$ . It turns out that in the zero-offset, high frequency case, this operator corresponds to the upward normal derivative operator.

$$\frac{\partial}{\partial n} \leftrightarrow i \frac{\omega}{c} \quad . \quad (3.5)$$

[Again, see Bleistein (1984) for the proof of this assertion.] We should view the use of  $\partial/\partial n$  as symbolic here. After all, the normal direction is not globally defined in  $\underline{x}$ , but only on the discontinuity surfaces. To be more precise, we should state that for a discontinuous function, such as  $\alpha(\underline{x})$ , multiplication of its Fourier transform by  $\pm i\omega/c$ , before Fourier inverting, asymptotically produces an array of Dirac delta functions with support on the discontinuity surfaces and weights equal to the jumps in  $\alpha(\underline{x})$  across those surfaces. The choice of sign is a matter of the direction in which the jump in  $\alpha(\underline{x})$  is to be computed. This output is equivalent to the normal derivative when we know the surface. Thus, the symbolism is justified.

Exercise 3.1. Show that the second derivative of the Heaviside step function is a doublet.

Exercise 3.2. Apply the differential operator in equation (2.1) (with  $v$  being the constant  $c$ ) to the "plane wave",

$$e^{i(k_1 x_1 + k_2 x_2 + k_3 x_3 - \omega t/c)}, \quad (3.6)$$

to derive equation (3.4).

Equations (3.4) and (3.5) which have been developed only for the constant  $c$  model hold as well for the variable background case if the data is zero-offset. The non-zero offset case requires a generalization involving the incident and reflected ray directions. We will discuss this extension later.

### 3.1.2. Extraction of information from bandlimited delta functions

One occasionally sees statements to the effect that the loss of low (high) frequencies in seismic data sets precludes effective use of Fourier inversion methods -- or at least precludes "accurate" inversions. In this section, we will demonstrate that while, indeed, some information is lost, much useful information remains.

We consider the simple model of a unit seismic pulse reflected from a horizontal layer at  $z = h$ . We ignore 3-D spreading, noise, attenuation, side swipe and many other effects in order to focus our attention on the single real world effect of bandlimiting. Later we will comment on the extension of these results to more realistic seismic models.

If the pulse is launched from  $z = 0$  at  $t = 0$  and the average propagation speed to the layer is  $c$ , then in an ideal (1-D) world the returned signal would be recorded as

$$U(t) = R \delta(t - t_0) \quad , \quad t_0 = 2h/c \quad . \quad (3.7)$$

Here,  $R$  denotes the reflection coefficient at the layer.

We wish to analyze the effect of losing the high and low end of the frequency band. To do this, we must examine the signal in frequency (Fourier) domain. Using causality we can write

$$U(t) \rightarrow u(\omega) = \int_{-\infty}^{\infty} e^{i\omega t} U(t) dt = \int_0^{\infty} e^{i\omega t} U(t) dt \quad (3.8)$$

From our model data, we then obtain

$$u(\omega) = \int_0^{\infty} e^{i\omega t} R \delta(t - t_0) dt = R e^{i\omega t_0} \quad , \quad (3.9)$$

with  $t_0$  given by (3.7).

Note that while the temporal quantity,  $t$ , is constrained to be positive by causality, the circular frequency,  $\omega = 2\pi f$ , can be negative. This "extra" information is merely a mathematical artifact, for since  $U$  is real in (3.7), it follows from (3.8) that

$$u(-\omega) = u^*(\omega) \quad , \quad (3.10)$$

with (\*) denoting complex conjugate. Hence, the negative frequency information is already determined by the positive frequency information. In filtering our seismic traces, we must take the negative frequencies into account in a manner consistent with (3.10).

The physical bandlimiting has four causes:

- (1) the "earth filter",
- (2) the equipment generating the probing signal, and
- (3) the receiver array,
- (4) intermediate seismic processing or "preprocessing".

However, in processing the observed data, we need only empirically decide on the usable bandwidth in our data and design a suitable bandpass filter. (This decision can be made by studying the Fourier magnitude traces.)

Thus, we model the net band-limiting effect as a bandpass filter applied to the seismic data. If we denote our real valued filter by  $F(\omega)$ , then our filtered trace becomes

$$u_B(\omega) = F(\omega) u(\omega) \quad . \quad (3.11)$$

Here, we use the subscript, B, to stand for "bandlimited." In order to keep our t-domain signal real, we impose the constraint (3.10) on the bandlimited trace. Since F is real, we find

$$F(-\omega) = F(\omega) \quad , \quad (3.12)$$

so that F is an even function. That is, we must select our bandpass filter, F, as a real, even function of  $\omega$  in order to ensure the proper extension to negative frequencies.

Exercise 3.3. Establish (3.10).

Exercise 3.4. Establish (3.12).

The simplest even bandpass filter is the "boxcar" filter:

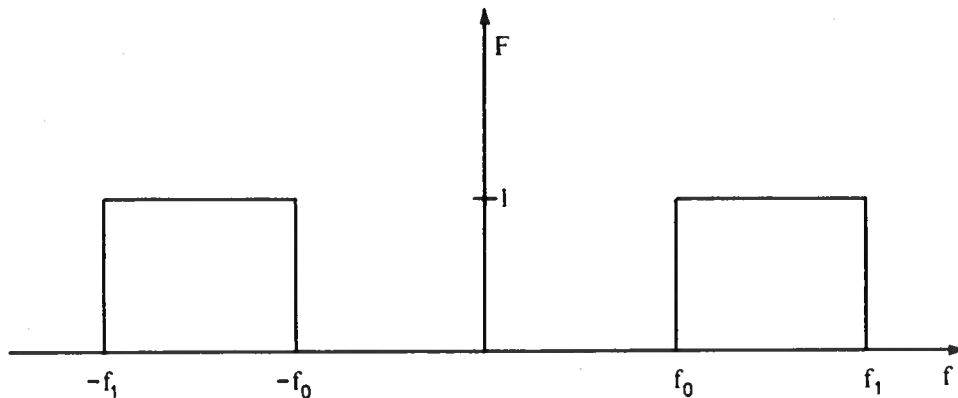


Figure 3.1. The Boxcar Filter

Here, we have introduced the physical frequency  $f$  (Hz) in place of the circular frequency  $\omega$ . This is a slight abuse of notation in that the function previously denoted by  $F(\omega)$  has now been set equal to  $F(f)$  rather than to  $F(2\pi f)$ . This will not play a crucial role in our analysis below.

In actual data processing, one would taper the ends of the boxcar to diminish "ringing", but for our present goal of illustrating basic ideas, the boxcar is adequate and provides analytic simplicity. In fact, if we choose  $F$  as the boxcar, and introduce a time delay,  $t_0 = 2h/c$ , through the equation

$$T = t - t_0 = t - 2h/c, \tag{3.13}$$

we can readily transform up back to time domain to obtain,

$$U_B(t) = R \frac{\sin 2\pi f_1 T - \sin 2\pi f_0 T}{\pi T} , \quad (3.14)$$

or alternately,

$$U_B(t) = 2R \sin \left[ \pi(f_1 - f_0)T \right] \cos \left[ \pi(f_1 + f_0)T \right] \quad (3.15)$$

Exercise 3.5. Noting the definition (3.13), establish (3.14).

Exercise 3.6. Establish (3.15).

From these results, a number of facts follow. We state them as a series of exercises.

Exercise 3.7. For the boxcar filter, show that  $U_B$  has a maximum at  $T = 0$  equal to

$$U_B(2h/c) = 2 R \left[ f_1 - f_0 \right] . \quad (3.16)$$

Exercise 3.8. For the boxcar filter, show that the zeroes nearest the origin of  $U_B$  are given by

$$T_1 = \pm \frac{1}{2(f_1 + f_0)} , \quad (3.17)$$

Exercise 3.9. Show that the next zeroes are given by

$$T_2 = \pm \min \left[ \frac{1}{f_1 - f_0}, \frac{3}{2(f_1 + f_0)} \right] \quad (3.18)$$

Exercise 3.10. Show that beyond  $T_2$ , we have the bounds

$$|U_B(t)| \leq \frac{2}{\pi T_2}, \quad \left| \frac{U_B(t)}{U_B(0)} \right| \leq \pi. \quad (3.19)$$

Equation (3.15) shows that we get a peak at a time equivalent to the correct reflector location. Thus, ideally, despite the loss of high and low frequencies, by graphing  $U_S$ , we image an isolated reflector at the correct location (relative to our reference profile).

We now show that an estimate of the reflection strength can also be made from bandlimited data. First note that the cutoff frequencies,  $f_0$  and  $f_1$ , are picked by the analyst according to the actual frequency content of the data (we are still ignoring the fact that in practice the frequency window will be tapered to zero). Thus, in light of equation (3.16), we need only divide the recorded amplitude by the known quantity  $2[f_1 - f_0]$  to obtain the reflection strength,  $R$ .

Exercise 3.11. Show that for non-box filters, this divisor is replaced by  $2A$ , where  $A$  is the area under the frequency filter,  $F(f)$  for  $0 < f < \infty$ .

We have concluded that, in our simple model, despite the loss of low and high frequencies, much useful information remains: we can estimate the relative location and strength of reflectors. There is no doubt that these

conclusions are tempered by the many factors ignored in our simple pedagogical model. Nonetheless, the concepts exposed do explain how it is that we can "see" reflectors on seismic sections despite the bandlimited nature of our data. Moreover, we are encouraged to think that amplitude information can help us to estimate earth parameters.

The remaining issues in ideal 1-D bandlimited data extraction are:

- (1) wavelet compression,
- (2) wavelet sidelobe height,
- (3) long range fall-off (ringing) of the wavelet.

Since this is not a treatise on either Fourier analysis or filtering, we will just state some rough results. None of them are very profound.

Wavelets become more compressed as the center frequency of the band is increased. This corresponds to the obvious fact that the higher the frequencies, the better the resolution. Since there is always a high frequency limit on the band, there are always beds too thin to be resolved, curvatures too great to be accurately imaged, etc. Often the changes in character of the wavelet and the "big picture" provide warning that our bandlimited data extraction is not to be trusted.

Decrease in wavelet sidelobe height is associated with increased percentage bandwidth (bandwidth relative to center frequency). This follows from (3.18, 19). If the band is too narrow we get the "picket fence" phenomenon which prevents us from distinguishing the main lobe from the side lobes.

From equation (3.14), we see that the boxcar filter has a long range

fall-off factor of  $1/T$ . In general, the smoother the wavelet, the more rapid the fall-off. For example, trapezoidal tapering gives a  $1/T^2$  fall-off, while smoothing the corners gives (at least) a  $1/T^3$  fall-off. A sine-squared taper (cubic fall-off) is a popular choice (Dale Stone, pers. comm.; Paul Stoffa, pers. comm.).

Similar concepts can be used to analyze 3-D waves. Once again, bandlimited inversion gives sinc-like approximations to the ideal delta function with peak at the reflector location and strength in known proportion to the reflection strength. However, in three dimensions, the derivation of the results requires high frequency approximations. As explained earlier, this is not a serious restriction in the geophysical context. We postpone these matters until we have derived some actual inversion algorithms, also see Bleistein (1984) and Mager and Bleistein (1978).

We remind the reader about the effect of the missing portions of the frequency spectrum. We have already indicated how the loss of high frequency information entails a loss of resolution. We now assert that the loss of the low frequency information implies a degradation of the over-all statistics of the data -- for example, that the overall mean or trend is lost. This can be seen at once by putting  $\omega$  equal to zero in the Fourier transform relation (3.8). Similarly, by differentiating (3.8), we can see that the "moments" (equivalently the variance, kurtosis, etc.) of  $U$  are degraded by the missing low frequency data.

We caution the reader about the visual interpretation of output sections. The fact that there are missing high frequencies is apparent to the eye -- reflectors have sidelobes, etc. The fact that there are missing low frequencies is less apparent. The explanation is that the output

section does contain low frequency information. Unfortunately, it is only the information that we have put in ourselves rather than additional information about the actual subsurface environment! Recall that our formulation requires specification of a reference profile. This profile contains low frequency information and this information is faithfully reproduced in the output section. In analyzing the output of our inversions, we must remember that the output trend information is nothing more than the reference velocity profile that we, ourselves, gave as input. Only the fluctuations around this trend constitute new (i.e. previously obscured) information.

In processing for the fluctuations around the assumed trend, we feel strongly that one should not attempt to replace the missing frequencies by theoretical extrapolation from the observed data. We feel it is important to make a judgement about the extent of the usable bandwidth and then to avoid processing the recorded information outside this bandwidth. Inserting "pure noise" into a migration/inversion algorithm is a good way to cause instability in an otherwise robust procedure, see Clayton and Stolt (1981).

In summary, then, we assert that for most of the length scales of interest in seismic exploration, seismic data is high frequency data. By exploiting the features of high frequency band limited functions, we can extract information about the discontinuity surfaces -- the reflectors -- in the subsurface, such as their location and the increment in earth parameters across them. This extraction process is facilitated by increased center frequency, increased percentage bandwidth and tapering, standard for any Fourier domain processing.

### 3.2. Effect of linearization

Even within the constraints of the Born approximation, careful analysis of the output allows us to partially correct our parameter estimates for the effects of linearization. We will demonstrate that here.

Once again, in order to present the salient points most clearly, we analyze a simple model: consider a suite of zero offset experiments done over a single horizontal reflector at depth  $h$ . Thus, the true velocity field can be written as

$$v = c + \Delta c H[z - h] \quad , \quad (3.20)$$

where  $\Delta c$  represents the jump in velocity across the reflector and  $H$  represents the Heaviside unit step function.

We now suppose that we have solved the Born integral equation (2.16) for  $\alpha$  in terms of the observed scattered field. A straightforward manipulation of the perturbation equation (2.6) leads to the following expression for  $\alpha$  in terms of  $\Delta c$ :

$$\alpha = \left[ \left[ \frac{1}{1 + \Delta c/c} \right]^2 - 1 \right] H [z - h] \quad . \quad (3.21)$$

When  $\Delta c$  takes on the value,  $-c$ , we see that the above expression becomes infinite! Of course, a value of  $\Delta c$  that is of the order of the background velocity  $c$  blatantly violates our perturbation assumption. The truth is, that after making the Born approximation, the naive use of equation (2.6) is no longer justified. Since we have linearized our integral equation, if we

wish to analyze the theoretical output of the algorithm then we should only use the linear approximation to (2.6). From either (3.21) or (2.6) itself, it is easy to derive the linear approximation,

$$\alpha_L = - \frac{2\Delta c_L}{c} H[z - h] , \quad (3.22)$$

for the expected output from the linearized integral equation. We have placed the subscript, L, on  $\Delta c$  to acknowledge that the algorithm is not perfect. That is,  $\Delta c$  is the true velocity jump, while  $\Delta c_L$  is the estimated jump from the algorithm. From (3.22), it follows at once that the estimated velocity jump is given in terms of the perturbation by:

$$\Delta c_L = - \frac{c\alpha_L}{2} \quad (3.23)$$

For the zero offset model, the input (which is not linearized!) is proportional to the normal incidence reflection coefficient,

$$R = \frac{(c + \Delta c) - c}{(c + \Delta c) + c} = \frac{\Delta c}{2c + \Delta c} . \quad (3.24)$$

We may think of the algorithm linearizing this to

$$R_L = \frac{\Delta c_L}{2c} \quad (3.25)$$

Thus, to compensate for the effects of linearization, we equate  $R_L$  to R:

$$\frac{\Delta c}{2c + \Delta c} = \frac{\Delta c_L}{2c} \quad (3.26)$$

On the one hand, this gives a correction to the "raw"  $\Delta c$  given by (2.24):

$$\Delta c = \frac{1}{\frac{1}{\Delta c_L} - \frac{1}{2c}} \quad (3.27)$$

and on the other hand,

$$a_L = -4R_L H[z - h] \quad (3.28)$$

so that the expected output from the algorithm is four times the reflection coefficient -- at least to first order.

Later, by applying our inversion operators to Kirchhoff approximate data, rather than to Born approximate data, we will see that, in fact, the ability to overcome the effects of linearization, as we have here, is not so surprising. We will find there that the output produces the fully nonlinear reflection coefficient, rather than just its linearized approximation as shown above. Of course, this requires that the background approximation above the reflector -- the surface where  $\alpha$  jumps -- is close to the true sound speed and that multiples from reflectors above the one in question do not degrade the output near the given reflector. These requirements are equivalent to small perturbations above the test reflector. Thus, the Born approximation is not completely avoided. However, with these caveats in place, the estimate of sound speed variation on the given reflector will not be constrained to be small. For non-zero offset, determination of the

reflection coefficient alone does not immediately lead to an estimate for  $\Delta c$ , but it is the crucial result needed to obtain such an estimate.

Equation (3.28) is an important adjunct to the practical implementation of the zero offset Born algorithm. However, it relies on the data having the correct scale (usually estimated from a well understood horizon).

Exercise 3.12. Why does knowledge of the non-zero offset reflection coefficient not imply the value of the velocity jump?

Exercise 3.13. Suppose that a set of seismic data has had a large scale factor inserted (this can happen, for example, when an integer FFT routine is applied to the data and the compensating scale factor is omitted). Can we still rely on (3.27) to be more accurate than (3.23)?

Recall that for the zero-offset, high frequency case, we process for the normal derivative of  $\alpha$  instead of for  $\alpha$  itself. Taking this normal upward and taking account of the two way time we can see that for our present simple model, introduction of the factor

$$\frac{1}{4} \cdot \frac{2i\omega}{c} = \frac{i\omega}{2c} \quad (3.29)$$

in frequency domain produces the reflectivity function; that is, the singular function of the reflector scaled by its reflection coefficient. We denote this function by  $\beta$ . In the high frequency regime, we see that it is related to  $\alpha$  by the equation,

$$\beta = \frac{1}{4} \frac{\partial \alpha}{\partial n} \quad (3.30)$$

Note that in the zero-offset model, the observed data is recorded at the two-way travelttime. To compensate for this, we have replaced  $c$  by  $c/2$  in adapting (3.5) for use in (3.29).

Our present results generalize to the case of many non-planar layers for the zero-offset case. However, they are not valid for nonzero source-receiver offset. We will obtain the correct generalization later.

### 3.3 Processing field data

We now wish to explicitly acknowledge some of the real world factors that damage our estimates of location and parameter values. These factors must be firmly kept in mind, lest in our enthusiasm for the elegance of the mathematics, we forget the limitations of our methods.

First of all, if the chosen reference velocity has serious errors, then the locations of the interfaces will be wrong. In turn, this will degrade the parameter estimates. We feel that naive iteration of the linear (Born) theory is not profitable. Real improvements come from a knowledgeable interpreter revising the estimate of the reference velocity by comparing the time section with the migrated inverted section.

Secondly, our analysis of the linearization effect only treated the case of an isolated reflector. Any strong "multiples" surviving the deconvolution of the data will appear on the migrated/inverted section as additional reflectors. This is an inevitable and unhappy result of linearizing an inherently nonlinear problem.

We have already acknowledged the resolution and trend problems arising from the band-limiting. In addition, we must recognize that weak reflectors will be lost in the noise. Finally, any model we adopt is a simplification of nature. For example, the model of reflection at abrupt layers is not accurate; the acoustic theory doesn't treat mode converted waves or the frequency dependent attenuation, etc. and etc.

We should not be unduly daunted by all these real world problems -- successful interpretations are made despite them -- but neither should we disregard them. Note that these issues affect all migration and inversion methods in the same way. In fact, many of them apply to the interpretation of unmigrated time sections as well.

#### 3.4. The effects of finite aperture and discretization

When an approximate solution to the Born integral equation can be derived, it consists of a integral over the source/receiver array (in the notation of Chapter 2, an integral over  $\xi$ ). Since this array is both discrete and finite in extent, we must deal with these restrictions in the implementation of our algorithms. Furthermore, the input to the algorithm also demonstrates discretization (digital recording) and limited aperture (finite length time records). Here, we wish to briefly explain how one deals with these four data restrictions. Full details are more conveniently given in terms of specific cases. Here we provide a brief (and unavoidably vague) introduction to these issues.

The finite length of the time records implies that we only have information about the subsurface down to finite depths. Furthermore, our reference velocity field allows us to make the (approximate) conversion of

time bounds to depth bounds explicitly. Thus, in the application of the inversion algorithm, we impose a "causality condition" to prevent wasting effort in an attempt to image deeper than we have information. Note that field time records are usually longer than the time records we process. The causality condition should be applied to the latter time!

The finite length of the ensemble of sources and receivers entails a degradation of information near the edges of the data set. The abrupt termination of reflectors causes "smiles." To avoid these diffraction-like artifacts, it is advisable to taper the first few and last few traces in the data set to zero (and perhaps the bottom of the trace, as well).

Another effect of the finite spatial aperture is the windowing problem: portions of the reflectors can not be imaged because their response occurs outside the window and is not recorded. In the implementation of the integration over the source/receiver parameter,  $\xi$ , the finite aperture is honored by merely truncating the theoretical infinite integral to a finite integral. In the "interior" of the section, this causes no problem because to produce a good image of a reflector segment, our recording array only has to "see" the region around the "specular" ray from this segment. We can often take advantage of this fact (making a virtue of necessity) to save computational effort. That is, in imaging a particular field point, it is desirable to limit the range of integration to the minimum necessary aperture for that point. However, such a notion requires a bound on the reflector dip -- otherwise speculars can emerge at arbitrarily distant offsets from the field point. But often, the time sections or other data provide (depth dependent) bounds on the maximum dip. In this case, we can limit the range of integration to a "little bit more" than the maximum specular offset. Empirically, the "little bit more" turns out to be a few

Fresnel zones (Sheriff, 1980 gives a brief, lucid treatment of the Fresnel zone concept). To determine the Fresnel zone for inversion, we must anticipate the abstract form of the inversion integral. For simplicity, we here treat only the linear array case (i.e. data collected only for  $\eta = 0$  and inversion computed for  $y = 0$ ). In this case, the form of the inversion integral is

$$\beta(x, z) = \iint A(x, z, \xi, \omega) e^{-i\omega\phi(x, z, \xi)} d\xi d\omega . \quad (3.31)$$

A Fresnel zone for  $\xi$  is defined as the differential value that produces a  $\pi/2$  increment in phase:

$$\omega d\phi = \pi/2 . \quad (3.32)$$

On switching to frequency in Hertz and re-arranging:

$$d\xi = \frac{1}{4f - \frac{\partial\phi}{\partial\xi}} . \quad (3.33)$$

Here,  $f_{-}$ , is a nominal low frequency in the band (e.g., the middle point of the left end taper of the filter  $F$  discussed above). The derivative in (3.33) is evaluated at the output point,  $(x, z)$ , and the  $\xi$  corresponding to the maximum dip specular from this point. That is, given a maximum dip at  $(x, z)$ , determine by tracing geometrical optics rays the value of  $\xi$  where reflection data from that dip will emerge at the upper surface. We find empirically that extension of the domain of summation by two Fresnel zones is adequate for numerical accuracy while extension by one is not. Thus, at that  $\xi$ -point, increment  $\xi$  by  $2d\xi$  with  $d\xi$  defined by (3.33). This defines

the limit of integration consistent with Fresnel zone considerations.

Exercise 3.14. In the next chapter, we will show that for the case of constant background sound speed and zero-offset source/receiver configuration,  $\phi$  is given by the two-way traveltime:

$$\phi = \frac{2}{c} \sqrt{(x - \xi)^2 + z^2} . \quad (3.34)$$

For the constant background ( $c = 1800$  m/s), zero-offset case, derive the minimum adequate integration range in  $\xi$  at output depth 600 m, if we are given that the magnitude of the maximum dip is  $30^\circ$  and that the data has been band passed filter with a 6-12-48-60 Hz filter. Here, the first two numbers define the range over which the filter rises from zero to full value and the last two define the range over which the filter decays from full value to zero. Answer:  
 $|\xi - x| = 200(1 + 2\sqrt{3}) = 893$  meters.

We turn from consideration of the finite aperture restrictions to the discretization effects. The discretization in time implies that there is a limit on the highest usable frequency -- the Nyquist limit:

$$f_+ < \frac{1}{2\Delta t} \quad (3.35)$$

Here  $\Delta t$  denotes the sampling rate and  $f_+$  is a nominal high frequency (e.g. the middle point of the right end taper of the band pass filter  $F$ ). Frequencies higher than the Nyquist limit are "aliased" onto lower frequencies. Fortunately, aliased frequencies are rejected in the field by

"anti-aliasing" filters, so we need not consider this restriction further.

On the other hand, the discretization in space provides a real challenge to the data processor. It turns out that even when there is no temporal aliasing (i.e. equation (3.35) is satisfied), there can easily be "spatial" aliasing. If we continue to assume that the inversion solution has the form of equation (3.31), the basic facts are easily derived. First, because of the sampling in the horizontal space dimension, we have the (spatial) Nyquist limit:

$$\frac{k_{\xi}}{2\pi} < \frac{1}{2\Delta\xi} \quad (3.36)$$

where  $\Delta\xi$  is the spatial sampling rate and  $k_{\xi}$  is the corresponding spatial wave number. This wave number can be expressed in terms of the phase in (3.31) as:

$$k_{\xi} = \omega \frac{\partial \phi}{\partial \xi} \quad (3.37)$$

Combining the last two equations leads to the condition:

$$\Delta\xi < \frac{1}{2 \frac{\partial \phi}{\partial \xi} f} \quad (3.38)$$

In the inversion process, the most convenient way to impose equation (3.38) is as a restriction on allowable dip or equivalently, allowable offset at given depth. In bad cases, this can conflict with the Fresnel zone requirement for successful imaging.

Exercise 3.15. Under the conditions of the previous exercise, compute the

maximum allowable spatial aperture for a CMP spacing of 15 meters. Given adequate observation apertures, can we successfully image under these conditions? Answer: Just barely. The maximum dip allowed at 600 m is  $33.8^\circ$

### 3.5. Summary

In this chapter, we have discussed the major issues arising from the constraints of the real world. We introduced the important theme of treating seismic records as high pass filtered data. We have also discussed:

- (1) The extraction of information from bandlimited data.
- (2) The estimation of parameters from the linearized theory.
- (3) The effects of finite aperture: the concept of causality with respect to the time dimension and the concept of Fresnel zone with respect to the lateral spatial dimension.
- (4) The effects of discretization: the concepts of temporal and spatial aliasing.

#### 4. Zero-offset Constant Reference Inversion

In this chapter, we study the derivation of the inversion algorithm first presented in the 1979 Geophysics paper, "Velocity inversion procedure for acoustic waves", by the authors of this monograph. Two later references that give further information are "Computational and asymptotic aspects of velocity inversion", Bleistein et al. (1985) and the text, "Mathematical Methods for Wave Phenomena", Bleistein (1984).

The model we study here is very simple and yet it is still the basis for much of the routine migration processing of seismic data. In addition to the general constraints discussed in the previous chapter, we here assume the background velocity field and the source/receiver configuration to be as simple as possible -- we assume that:

- (1) the background is a constant velocity and
- (2) the data is collected at zero-offset.

As remarked earlier, in actuality, CMP data is used to simulate zero-offset data.

It is interesting to note that two of the classic papers on migration were roughly contemporaneous with the work on velocity inversion described in this chapter: Schneider's "Integral formulation for migration in two and three dimensions", and Stolt's "Migration by Fourier transform", having appeared in the previous year. Although it was hardly apparent in 1979, in the ensuing years it has been shown that the three algorithms have much in common, see Cohen and Bleistein (1982), Cheng and Coen (1983) and Bleistein et al. (1985).

#### 4.1. Three dimensional algorithm

In this section, we will derive the Born inversion formula for zero offset data in a constant background sound speed and constant density medium. We begin from the Born integral equation (2.16) which we repeat here for the readers' convenience:

$$u_S(\omega, \underline{x}_g, \underline{x}_s) = \omega^2 \iiint d^3 \underline{x} \frac{g(\omega, \underline{x}, \underline{x}_g) g(\omega, \underline{x}, \underline{x}_s)}{c^2(\underline{x})} \alpha(\underline{x}) \quad (4.1)$$

Since we treat the case of zero-offset, we have

$$\underline{x}_s = \underline{x}_g = \underline{x}_o = (\underline{\xi}, 0) = (\xi_1, \xi_2, 0) \quad . \quad (4.2)$$

In addition, since the background sound speed is assumed to be constant,

$$c(\underline{x}) = c = \text{constant} \quad , \quad (4.3)$$

we can write down an explicit representation for the Green's function:

$$g(\omega, \underline{x}, \underline{x}_o) = \frac{e^{i\omega r/c}}{4\pi r} \quad , \quad r = |\underline{x} - \underline{x}_o| \quad . \quad (4.4)$$

Exercise 4.1. Establish the above expression for  $g$  by Fourier methods. Some may find it easier to establish the time domain representation,

$$G(t, \underline{x}, \underline{x}_o) = \frac{\delta(t - r/c)}{4\pi r} \quad . \quad (4.5)$$

With this result, we can write the simplified Born equation (4.1) as:

$$\iiint d^3 x \frac{e^{2i\omega r/c}}{(4\pi r)^2} \alpha(\underline{x}) = \left[ \frac{c}{\omega} \right]^2 u_S(\omega, \underline{\xi}) . \quad (4.6)$$

Here, we have shortened our notation for the zero-offset data vector, by writing,

$$u_S(\omega, \underline{\xi}) = u_S(\omega, \underline{\xi}, 0, \underline{\xi}, 0) . \quad (4.7)$$

We remind the reader that although the integral in (4.6) is formally written as being over all space, we have assumed that  $\alpha$  vanishes in the non-physical (air) region  $z < 0$ . Hence we can alternatively consider the region of integration as being over the half space representing the subsurface of the earth.

Exercise 4.2. In equation (4.6), the data,  $u_S$ , is written in frequency domain. This data arises from a function assumed to vanish identically for  $t < 0$ . It can be shown that this and finite energy implies that  $u_S$  is analytic in the upper half of the  $\omega$  plane and decays to zero there as  $|\omega| \rightarrow \infty$  (even exponentially in  $\text{Im } \omega$  as  $\text{Im } \omega \rightarrow \infty$ ) in this half plane. Assuming these properties, prove the converse:  $U_S$  vanishes for  $t < 0$ .

The integral in (4.6) is a convolution in the transverse spatial variables,  $x$  and  $y$ . Thus, a transverse Fourier transform is indicated. Unfortunately, in order to do this transform explicitly, we require the two-dimensional transform of the square of the Green's function:

$$h_1(\omega, \underline{K}, z) = \frac{1}{16\pi^2} \iint d^2\rho \frac{\exp\left[-i\underline{K}\cdot\underline{\rho} + [2i\omega/c]\sqrt{\rho^2 + z^2}\right]}{\rho^2 + z^2} \quad (4.8)$$

$$\underline{K} = (k_x, k_y) \quad , \quad \underline{\rho} = (x, y) \quad , \quad \rho^2 = x^2 + y^2 \quad .$$

Alas, the transform,  $h_1$ , is not known (to us, at least) in closed form. However, if we differentiate with respect to  $\omega$ , the required integral becomes the transform of the Green's function, itself -- but with  $c$  replaced by  $c/2$ . The appearance of the halved speed is quite natural. In the zero-offset model, the "specular" rays travel back and forth on the same path. Thus we can equivalently consider either "two way time" with the actual speed or "one way time" with halved speed. It is gratifying that the mathematics so closely mirrors the "exploding reflector" model used in migration, see Loewenthal, et al. (1976).

On carrying out the  $\omega$  differentiation, our inversion integral equation becomes

$$\iiint d^3x \frac{e^{2i\omega x/c}}{4\pi r} a(\underline{x}) = -2\pi i c^3 \frac{\partial}{\partial \omega} \left[ \frac{u_S(\omega, \xi)}{\omega^2} \right] \quad (4.9)$$

We now define the 2-D Fourier transform,

$$\hat{f}(\underline{K}) = \iint d^2\rho e^{2i\underline{K}\cdot\underline{\rho}} f(\underline{\rho}) \quad (4.10)$$

Here  $\underline{\rho}$  and  $\underline{K}$  are as above, but note that we have inserted a factor of 2 in the exponent of the transform kernel. This factor is not essential, but it makes the subsequent formulas a bit nicer. We note that in inverting a

transform with the 2 factor in the exponent, we have a  $1/\pi$  factor outside the inversion integral instead of the usual  $1/2\pi$  factor. Thus,

$$f(\underline{\rho}) = \frac{1}{\pi^2} \iint d^2\underline{K} e^{-2i\underline{K}\cdot\underline{\rho}} \hat{f}(\underline{K}) . \quad (4.11)$$

Exercise 4.3. Establish the inversion formulas for both the 1-D and 2-D Fourier transforms when a 2 factor is inserted in the exponent as in (4.10). The 2-D result should agree with (4.11).

On applying the indicated transform to (4.9), we obtain:

$$\int_0^\infty dz g_1(\omega, \underline{K}, z) \hat{a}(\underline{K}, z) = d(\omega, \underline{K}) \quad (4.12)$$

Here the kernel,  $g_1$ , is given by

$$g_1(\omega, \underline{K}, z) = \frac{1}{4\pi} \iint d^2\rho \frac{\exp \left[ 2i\underline{K}\cdot\underline{\rho} + [2i\omega/c] \sqrt{\rho^2 + z^2} \right]}{\sqrt{\rho^2 + z^2}} \quad (4.13)$$

and the "data",  $d$ , by

$$d(\omega, \underline{K}) = -2\pi i c^3 \frac{\partial}{\partial \omega} \left[ \frac{\hat{u}_2(\omega, \underline{K})}{\omega^2} \right] . \quad (4.14)$$

The kernel,  $g_1$  can be evaluated explicitly as

$$g_1(\omega, \underline{K}, z) = \frac{i}{4k_z} e^{2ik_z z} , \quad (4.15)$$

where the vertical wave number (technically half the vertical wavenumber),  $k_z$  is defined as

$$k_z = \begin{cases} \operatorname{sgn}(\omega) \sqrt{\omega^2/c^2 - K^2} , & |\omega| \geq cK , \\ i \sqrt{K^2 - \omega^2/c^2} , & |\omega| < cK . \end{cases} \quad (4.16)$$

It will be observed that in the remainder of the derivation only the regime,  $|\omega| > cK$ , will be required. The reason is that  $\alpha(\underline{x})$  can be reconstructed from its Fourier transform  $\hat{\alpha}(\underline{k})$  over real values of the  $\underline{k}$ -vector, only. This is important because data in the "evanescent" region,  $|\omega| < cK$  is physically unattainable.

We outline three alternate ways of deriving (4.15) in the following exercises.

Exercise 4.4. Introduce polar coordinates,

$$\underline{\rho} = \rho (\cos\theta, \sin\theta), \quad \underline{K} = K (\cos\phi, \sin\phi) , \quad (4.17)$$

and argue that  $g$  is independent of  $\phi$ . Then show that the  $\theta$  integration produces the Bessel function,

$$\int_{-\pi}^{\pi} d\theta e^{-2iK\rho\cos\theta} = 2\pi J_0(2K\rho) \quad ; \quad (4.18)$$

see Abramowitz and Segun (1965), equation 9.1.18. In the remaining  $\rho$  integral, make the substitution,

$$u = \sqrt{\rho^2 + z^2} \quad (4.19)$$

and observe that the resulting integral can be written as a linear combination of sine and cosine transforms, see Erdelyi, et al. (1953), equations 1.13(48) and 2.13(47). [Note: our editions have inadvertently omitted a square root symbol in the first of these results.]

Exercise 4.5. After completing the angular integral as above, alternatively evaluate the radial integral by use of Hankel transform tables, see Erdelyi, et al. (1953), equation 8.2(25).

After carrying out either of the above two approaches and attaining a result as simple as (4.15), it is natural to ask if there is not a less tedious way of obtaining the result. Indeed there is. Since the kernel of (4.9) is the free space Green's function with speed  $c/2$ , it satisfies the wave equation with speed  $c/2$  and source,  $\delta(x)\delta(y)\delta(z)$ . On carrying out the indicated transverse transforms on the wave equation, we find that  $g_1$  (4.15) satisfies the equation for the 1-D Green's function.

Exercise 4.6. Carry out the indicated reduction and solve the equation for 1-D Green's function to obtain (4.15).

Note: Integrals like this come up all the time. See Craig (1986) for a recent example. Can you do better than Craig using the method of the current exercise?

Using (4.15) in (4.12), we reduce the inversion integral equation to the following a 1-D integral equation for the lateral transform of  $\alpha$ :

$$\int_0^{\infty} dz e^{2ik_z z} \hat{\alpha}(\underline{K}, z) = -4ik_z d(\omega, \underline{K}) \quad (4.20)$$

The remaining integral is almost a Fourier integral and, indeed, the following observations allow us to write it as such:

- (1) Since  $\alpha(\underline{x}) = 0$  for  $z < 0$ , so is  $\hat{\alpha}(\underline{K}, z)$ ; hence we can extend the integral to  $-\infty$ . (It was convenient to reduce the interval to  $z > 0$  to allow writing  $z$  instead of  $|z|$  as required in the transform results cited in Exercises 4.4-6.)
- (2) As  $\omega$  varies from  $-\infty$  to  $-cK$  and from  $cK$  to  $+\infty$ ,  $k_z$  varies from  $-\infty$  to  $+\infty$ , and is thus a suitable conjugate Fourier variable to  $z$ .
- (3) In the regime,  $|\omega| > cK$ , we can use (4.16) to write  $\omega$  as a function of  $k_x$  and  $K$ :

$$\omega = \omega_0(K, k_z) = c \operatorname{sgn}(k_z) \sqrt{K^2 + k_z^2} = \operatorname{sgn}(k_z) \sqrt{k_x^2 + k_y^2 + k_z^2} \quad (4.21)$$

With these observations, we can invert (4.20) at once to obtain

$$\hat{\alpha}(\underline{K}, z) = \frac{4}{\pi i} \int_{-\infty}^{\infty} dk_z k_z e^{-2ik_z z} d(\omega_0, \underline{K}) \quad (4.22)$$

We have essentially solved our integral equation for  $\alpha$ ! All that remains to do is:

- (4) use (4.11) to invert the spatial transforms, thus writing  $\alpha$  in spatial variables;
- (5) use (4.14) to write  $d$  in terms of  $\hat{u}_S(\omega, \underline{K})$ ;
- (6) use (2.20) to write the transform,  $\hat{u}_S(\omega, \underline{K})$ , in terms of  $u_S(\omega, \underline{\xi})$ ;
- (7) write  $u_S(\omega, \underline{\xi})$  in terms of its inverse temporal transform, i.e., in terms of  $U_S(t, \underline{\xi})$ .

We follow this straightforward, but tedious, program in the following sequence of equations. First write  $\alpha$  in spatial variables:

$$\alpha(\underline{x}) = \alpha(\underline{\rho}, z) = \frac{4}{\pi^3 i} \int dk_z \iint d^2 \underline{K} e^{2i[\underline{K} \cdot \underline{\rho} - k_z z]} k_z d(\omega_0, \underline{K}) \quad (4.23)$$

Then replace  $d$ :

$$\alpha(\underline{x}) = -\frac{8c^3}{\pi^2} \iiint d^3 \underline{k} e^{2i[\underline{K} \cdot \underline{\rho} - k_z z]} k_z \frac{\partial}{\partial \omega} \left[ \frac{\hat{u}_S(\omega, \underline{K})}{\omega^2} \right] \Big|_{\omega = \omega_0} \quad (4.24)$$

Here, we have combined the  $k_z$  integral with the  $k_1, k_2$  (or  $k_x, k_y$ ) integrals as a triple integral over a 3-D  $\underline{k}$ . Next we undo the spatial transform of  $u_S$ :

$$\alpha(\underline{x}) = -\frac{8c^3}{\pi^2} \iint d^2\xi \iiint d^3k k_z \cdot \frac{\partial}{\partial \omega} \left[ \frac{1}{\omega^2} e^{i[2\underline{K} \cdot (\underline{\rho} - \underline{\xi}) - k_z z + \omega t]} U_S(\omega, \underline{\xi}) \right] \Big|_{\omega = \omega_0} \quad (4.25)$$

and then the temporal transform,

$$\alpha(\underline{x}) = -\frac{8c^3}{\pi^2} \iint d^2\xi \iiint d^3k k_z \cdot \frac{\partial}{\partial \omega} \left[ \frac{1}{\omega^2} \int_0^\infty dt e^{i[2\underline{K} \cdot (\underline{\rho} - \underline{\xi}) - k_z z + \omega t]} U_S(t, \underline{\xi}) \right] \Big|_{\omega = \omega_0} \quad (4.26)$$

Finally, we note that

$$\frac{\partial}{\partial \omega} \left[ \frac{1}{\omega^2} e^{i\omega t} \right] = \frac{1}{\omega^2} [it - 2/\omega] e^{i\omega t} \quad (4.27)$$

and obtain the inversion formula,

$$\alpha(\underline{x}) = \frac{8c^3}{\pi^2 i} \iint d^2\xi \iiint d^3k F(\underline{k}) e^{2i[\underline{K} \cdot (\underline{\rho} - \underline{\xi}) - k_z z]} \int_0^\infty dt t U_S(t, \underline{\xi}) \frac{e^{i\omega_0 t}}{\omega_0^2} \left[ 1 + \frac{2i}{\omega_0 t} \right] \quad (4.28)$$

where once again,

$$\omega_0 = ck \operatorname{sgn}(k_z) = c \sqrt{K^2 + k_z^2} \operatorname{sgn}(k_z) . \quad (4.29)$$

Formula (4.28) provides a wide band inversion for the perturbation,  $\alpha$ . Although we have never implemented this formula ourselves, it is apparent that its structure is similar to Stolt's 1978 k-f migration formula.

Thus, starting from (4.6), the Born approximation of the upward scattered wave in a constant background soundspeed, constant density medium, we have derived a full bandwidth inversion formula (4.28) for  $\alpha(\underline{x})$ . The derivation relied on Fourier transform theory and the convolution theorem.

#### 4.2. High frequency approximations

At this point, we wish to exploit the high frequency nature of ordinary seismic data to simplify the inversion processing. We return to equation (4.22) and before inverting the transform, we introduce the factor derived in equation (3.29) that provides edge sharpening and (for zero-offset data) converts  $\alpha$  into the reflectivity function,  $\beta$ . That is, in (4.22), we multiply on the right by  $i\omega/2c$  and replace  $\hat{\alpha}$  by  $\hat{\beta}$  on the left. The result is

$$\int_0^{\infty} dz e^{2ik_z z} \hat{\beta}(\underline{K}, z) = \frac{2\omega k_z}{c} d(\omega, \underline{K}) . \quad (4.30)$$

We can now repeat the steps that led from (4.20) to (4.28). Alternatively, multiply by  $i\omega/2c$  on the right in (4.28) and replace  $\alpha$  by  $\beta$  on the left. We then drop the lower order term in  $\omega$  --  $2i/\omega_0 t$  -- in (4.28) to obtain

$$\beta(\underline{x}) \sim \frac{4c}{\pi^2} \iint d^2\xi \iiint d^3k \frac{|k_z|}{k} e^{2i[\underline{K} \cdot (\underline{\rho} - \underline{\xi}) - k_z z]} \cdot \int_0^\infty dt t U_S(t, \underline{\xi}) e^{i c k t \operatorname{sgn}(k_z)} . \quad (4.31)$$

Here, we have used (4.29) to eliminate  $\omega_0$ .

Exercise 4.7. Establish (4.31) by following the outlined steps of the previous paragraph.

Because of the relation (4.29), the bandlimiting in frequency is equivalent to bandlimiting in  $k$  -- the magnitude of the 3-vector,  $(\underline{K}, k_z)$ . We introduce the polar coordinates,

$$\underline{K} = k(\cos \phi, \sin \phi) \sin \theta, \quad k_z = k \cos \theta, \quad (4.32)$$

and

$$\underline{\rho} - \underline{\xi} = r(\cos \lambda, \sin \lambda) \sin \mu, \quad z = r \cos \mu. \quad (4.33)$$

Thus, as in (4.29),

$$k = \sqrt{K^2 + k_z^2}, \quad (4.34)$$

and we also have,

$$r = |\underline{\rho} - \underline{\xi}|^2 + z^2 = (x - \xi)^2 + (y - \eta)^2 + z^2 . \quad (4.35)$$

Carrying out stationary phase in the angular variables, with  $k$  (i.e.,  $\omega$ ) as the formal large parameter, we obtain

$$\beta(\underline{x}) \sim -\frac{8cz}{\pi} \iint \frac{d^2 \xi}{r^2} \int_0^\infty dt t U_S(t, \underline{\xi}) \int_0^\infty dk k F(k) \sin[ck\{t - 2r/c\}] . \quad (4.36)$$

Here, we have introduced a filter analogous to that discussed earlier in Chapter 3 in order to make explicit the high pass nature of our data,  $U_S$  -- how else could we justify stationary phase?

Exercise 4.8. Establish this result by the method of stationary phase.

Exercise 4.9. What happens if you do not switch to polar coordinates and instead do stationary phase in the original  $\underline{K}$  variables?

Exercise 4.10. "Simplify" the above expression for  $\beta$  by doing the  $k$  integral explicitly (for a box car filter).

For purposes of processing actual data with the FFT, it helps to write the sine function in (4.36) as

$$\sin[ck\{t - 2r/c\}] = \text{Im } e^{ick(t - 2r/c)} , \quad (4.37)$$

and then our algorithm becomes

$$\beta(\underline{x}) \sim - \frac{8cz}{\pi} \operatorname{Im} \iint \frac{d^2 \xi}{r^2} \int_0^\infty dk k F(k) e^{-2ikr} \int_0^\infty dt t U_S(t, \underline{\xi}) e^{ickt} . \quad (4.38)$$

Finally we introduce the temporal frequency,

$$f = \frac{|\omega|}{2\pi} = \frac{ck}{2\pi} , \quad (4.39)$$

to obtain

$$\beta(\underline{x}) \sim - \frac{32\pi z}{c} \iint \frac{d^2 \xi}{r^2} \operatorname{Im} \int_0^\infty df f F(f) e^{-2\pi if(2r/c)} \int_0^\infty dt t U_S(t, \underline{\xi}) e^{2\pi ift} . \quad (4.40)$$

This form of the algorithm is suitable for processing 3-D (areal) data sets.

The steps are:

- (1) Forward FFT over time of weighted data.
- (2) Inverse FFT of filtered data.
- (3) Quadrature over receiver array.

All our algorithms will have this general structure.

Exercise 4.11. Recognize that the factor of  $t$  in the time integral of the last equation can be replaced by a differentiation in  $f$  and do an integration by parts in  $f$  to obtain,

$$\beta(\underline{x}) \sim - \frac{64\pi z}{c^2} \iint \frac{d^2 \xi}{r} \operatorname{Im} \int_0^\infty df f F(f) e^{-2\pi i f(2r/c)} \int_0^\infty dt U_S(t, \underline{\xi}) e^{2\pi i f t} \quad (4.41)$$

which is an alternate processing form of the inversion algorithm. Hints: Exploit the high frequency assumption and use the fact that the filter tapers smoothly to zero.

We note that the two forms just stated for the processing algorithm differ only by trading a factor of  $t$  for the corresponding two-way traveltime,  $2r/c$ . This trade-off makes intuitive sense in the high frequency regime.

While the last two forms of the algorithm are suitable for computer implementation, they are not the most convenient form for theoretical work.

Exercise 4.12. In (4.36) use Euler's formula for the sine function and the evenness of the filter function to show that

$$\beta(\underline{x}) \sim \frac{8iz}{\pi c^2} \iint \frac{d^2 \xi}{r} \int_{-\infty}^\infty d\omega \omega F(\omega) e^{-2i\omega r/c} \int_0^\infty dt U_S(t, \underline{\xi}) e^{i\omega t} \quad (4.42)$$

Thus, starting from a full bandwidth inversion formula for  $\alpha$  (4.28), we have derived an inversion formula for the reflectivity function,  $\beta$ . That formula uses only high frequency zero offset data gathered over a surface.

### 4.3. Two-and-one-half dimensional limit

Although 3-D surveys are becoming more common, the typical seismic data set is still a set of traces gathered along a line. In such a case it is not possible to obtain a full 3-D image of the subsurface. The self-consistent model for a linear survey is a subsurface that does not vary in the direction orthogonal to the survey. With a field data set, this assumption will not be true and reflections due to out-of-plane reflectors gives rise to the phenomenon known as "side swipe." However, given only a line of data, we must make some assumption about the data that would have been collected on parallel lines and the universal choice for that assumption is that every line would give the same data as the one observed.

In some of the older migration work, the above "cylindrical earth" assumption was augmented by an assumption of line sources extending in the direction orthogonal to the survey line. This reduces the mathematical model to a two-dimensional one, but has the cost of replacing the actual quasi-spherical spreading of the signal by quasi-cylindrical spreading. Such a replacement obviously would have an adverse effect on the amplitude information in the signal and hence on the derived parameter estimates. For this reason, we retain our point source model of the actual 3-D sources. We call this combination of 3-D wave propagation into a 2-D earth the 2.5-D wave model. The notion of "two-and-one-half-dimensional" modeling is explicated in Bleistein (1986). Other authors who address this type of specialization are Cerveny, et al. (1977), Cerveny and Hron (1980), Ben-Menachem and Beydoun (1985), Cerveny and Ravrinda (1971), Kennett (1983), and Ursin (1983). Its use in inversion is made explicit in Bleistein, et al. (1985b), but it has, in fact, been used both by us and

others for many years.

It turns out that in our inversion work, the 2.5-D model is no harder to treat than the less realistic 2-D (line source) model. Thus, we pay no penalty for adopting the better model. Alas, the same is not true universally in geophysics. In finite difference forward modeling, there is no question that 2-D is much less CPU intensive than 3-D modeling. However, the work of Bleistein (1986) may help in reducing the forward modeling penalty.

The process of adapting our previously derived 3-D inversion formulas to the 2-D earth model to obtain the 2.5-D inversion formulas is simple. We observe that the 2-D earth assumption amounts to assuming that  $U_S$  is independent of the transverse coordinate,  $\eta$ . Thus, the only  $\eta$  dependence occurs in the phase, and so in (4.40) we can calculate the  $\eta$  integral,

$$I = \int d\eta \frac{e^{-4\pi i f r/c}}{r^2}, \quad r^2 = (x - \xi)^2 + (y - \eta)^2 + z^2 \quad (4.43)$$

in isolation. We once more exploit the high frequency assumption to do this integral by stationary phase.

Exercise 4.13. Show that

$$I \sim \frac{1 - i}{2} \sqrt{\frac{c}{f}} \frac{1}{r^{3/2}} e^{-4\pi i f r/c}, \quad (4.44)$$

where now (and henceforward in our 2.5-D work),

$$r^2 = (x - \xi)^2 + z^2 \quad . \quad (4.45)$$

Exercise 4.14. Show that for a complex number  $z$ ,

$$\text{Im}(1 - i)z = - (\text{Re } z - \text{Im } z) \quad , \quad (4.46)$$

and hence, for the 2.5-D model, the "processing" form of the inversion algorithm is

$$\beta(\underline{x}) \sim \frac{16\pi z}{\sqrt{c}} \int \frac{d\xi}{r^{3/2}} (\text{Re} - \text{Im}) \int_0^\infty df \sqrt{f} F(f) e^{-2\pi i f(2r/c)} \quad . \quad (4.47)$$

$$\int_0^\infty dt t U_S(t, \xi) e^{2\pi i f t} \quad .$$

where now  $\underline{x}$  is the 2-vector,  $(x, z)$ , and  $r$  is as in (4.44) above.

Exercise 4.15. Show that the "alternate processing" form of the 2.5-D inversion algorithm analogous to (4.40) for 3-D inversion is

$$\beta(\underline{x}) = \frac{32\pi z}{c^{3/2}} \int \frac{d\xi}{\sqrt{r}} (\text{Re} - \text{Im}) \int_0^\infty df \sqrt{f} F(f) e^{-2\pi i f(2r/c)} \quad . \quad (4.48)$$

$$\int_0^\infty dt U_S(t, \xi) e^{2\pi i f t} \quad .$$

Exercise 4.16. Show that the "theory" form of the 2.5-D inversion algorithm analogous to (4.41) for the 3-D inversion is

$$\beta(\underline{x}) \sim \frac{8z}{c\sqrt{\pi c}} \int \frac{d\xi}{\sqrt{r}} \int_{-\infty}^{\infty} d\omega \sqrt{i\omega} e^{-2i\omega r/c} \int_0^{\infty} dt U_S(t, \xi) e^{i\omega t} , \quad (4.49)$$

$$\sqrt{i\omega} = \sqrt{|\omega|} e^{i\pi/4 \operatorname{sgn}(\omega)}$$

Exercise 4.17. Make the 2.5-D assumption in the wide band formula and then specialize your answer to the high frequency regime as a check.

Exercise 4.18. Make the 2.5-D assumption just before the 2-D angular stationary phase calculation above and then do 1-D angular stationary phase to obtain an alternate derivation of the 2.5-D processing formula.

Exercise 4.19. Examine the 1.5-D limit, that is, the case in which only one experiment is done and we adopt the model of a stratified earth. You can start either from the 3-D or the 2.5-D forms of the inversion algorithm.

We have now provided formulas for constant background sound speed, constant density, zero offset 2.5-D inversion. These are the formulas used to process a single line of seismic data.

#### 4.4. Verification for model data

We will develop some analytical checks on the inversion formulas we have derived. First, we will consider the case of a single planar reflector and then a more general curved reflector for which we use the Kirchhoff

approximation to represent the upward propagating wave. We note that neither check evokes the Born approximation -- that is, our checks do not assume that the reflector is weakly contrasting with the reference.

#### 4.4.1. Verification for a horizontal plane

The zero-offset ("back scattered") field due to a horizontal reflector at depth  $h$  is asymptotically given by

$$U_S(t, \underline{\xi}) = R \frac{\delta(t - 2h/c)}{8\pi h} . \quad (4.50)$$

The exact solution has a second term involving a step function. Thus, in the frequency domain we have retained a term which is  $O(1)$  in  $\omega$  as  $|\omega| \rightarrow \infty$  and neglected a term that is  $O(1/|\omega|)$  as  $|\omega| \rightarrow \infty$ . In this equation,  $c$  denotes the constant speed above the reflector and  $R$  denotes the reflection coefficient characterizing the medium below the reflector. More precisely, for our zero offset model, we may write

$$R = \frac{c_1 - c}{c_1 + c} = \frac{\Delta c}{2c + \Delta c} , \quad (4.51)$$

where  $c_1$  and  $\Delta c$  respectively denote the speed below the reflector and the jump in speed across the reflector. On inserting the data (4.50) into the "theory" form of our 3-D algorithm (4.42), and exploiting the delta function in  $t$ , we obtain

$$\beta(\underline{x}) \sim \frac{8iz}{\pi c^2} \iint \frac{d^2 \xi}{r} \int d\omega \omega F(\omega) e^{-2i\omega r/c} R \frac{e^{2i\omega h/c}}{8\pi h} .$$

(4.52)

$$= \frac{izR}{\pi^2 c^2 h} \int d\omega \omega F(\omega) e^{2i\omega h/c} \iint d^2 \xi \frac{e^{-2i\omega r/c}}{r}$$

Exercise 4.20. Do stationary phase in the source/receiver locations  $\xi$  to show that the stationary point is  $\underline{\xi} = \underline{x}$  and hence

$$\beta(\underline{x}) \sim \frac{Rz}{\pi ch} \int d\omega F(\omega) e^{-2i\omega(z-h)/c} .$$

(4.53)

Hint:

$$e^{-i\pi/2 \operatorname{sgn}(\omega)} = -i \operatorname{sgn}(\omega)$$

(4.54)

If the filter,  $F$ , were absent from our integral, then the last integral would produce a delta function:

$$\beta(\underline{x}) = \frac{Rz}{\pi ch} \pi c \delta(z - h) = R \delta(z - h) .$$

(4.55)

This would be the "correct" result! That is, our inversion formula would have reconstructed the surface and the reflection coefficient.

To honor the bandlimited nature of our data and of our result, we write instead,

$$\beta(\underline{x}) \sim R \delta_B(z - h) \quad (4.56)$$

where the subscript B denotes bandlimited. By this notation, we mean that the result is a sinc-like function that peaks on the reflector. The peak value is proportional to the reflection coefficient. In fact, the proportionality factor can be evaluated in terms of the filter function and thus the reflection coefficient may be estimated.

Exercise 4.21. Suppose that  $F(f)$  is a nonnegative, even filter function and, that  $\delta_B(2(z-h)/c)$  is its inverse transform. Show that the peak value of this function at  $z = h$  is just  $2A$ , where  $A$  is the area under the  $F(f)$  for  $f$  positive and that this bandlimited delta function has the dimension  $(\text{time})^{-1}$ .

Exercise 4.22. Carry out the analogous check for the 2.5-D case. That is, insert the solution (4.49) into the inversion formula (4.48) and obtain the result (4.54).

We have now checked that for a single flat plane, the inversion formula asymptotically yields a bandlimited delta function scaled by the exact (nonlinear in  $\Delta c$ ) reflection coefficient. The inversion formula has converted the arrival time of the impulse from the reflector into a depth consistent with two way traveltime at the background sound speed,  $c$ .

#### 4.4.2. Kirchhoff scattering data

We now consider a single more general curved reflector,  $S$ . We use the Kirchhoff approximation (Bleistein, 1986) to approximate this data. We emphasize that the Born approximation of weak contrast is not made in deriving this formula:

$$u_S(\omega, \underline{x}_g, \underline{x}_s) \sim i\omega \int_S dS \, R \left[ \tau_{sn} + \tau_{gn} \right] g(\omega, \underline{x}, \underline{x}_g) g(\omega, \underline{x}, \underline{x}_s) , \quad (4.57)$$

where the  $g$ 's denote the WKB approximations,

$$\begin{aligned} g(\omega, \underline{x}, \underline{x}_g) &\sim A(\underline{x}, \underline{x}_g) e^{i\omega\tau(\underline{x}, \underline{x}_g)} , \\ g(\omega, \underline{x}, \underline{x}_s) &\sim A(\underline{x}, \underline{x}_s) e^{i\omega\tau(\underline{x}, \underline{x}_s)} , \end{aligned} \quad (4.58)$$

with the  $\tau$ 's being conoidal solutions of the eikonal equation and the  $A$ 's satisfying the first transport equation. Moreover, we have used the notations,

$$\tau_{sn} = \hat{n} \cdot \nabla\tau(\underline{x}, \underline{x}_s) , \quad \tau_{gn} = \hat{n} \cdot \nabla\tau(\underline{x}, \underline{x}_g) , \quad (4.59)$$

with  $\hat{n}$  the upward normal on  $S$ . We also introduce  $\tau_{tn}$ , the normal derivative of the transmitted phase just below the surface as

$$\tau_{tn} = \text{sgn}(\tau_{sn}) \sqrt{\tau_{sn}^2 + \left[ \frac{1}{c^2} \right]} . \quad (4.60)$$

Here the brackets denote the jump across the surface (value below minus

value above). With this notation we can conveniently express the reflection coefficient,  $R$ , in (4.57) as

$$R = \frac{\tau_{sn} - \tau_{tn}}{\tau_{sn} + \tau_{tn}} . \quad (4.61)$$

**Exercise 4.23.** Specialize the Kirchhoff scattering data formula to the case of backscatter with constant reference speed to obtain

$$u_S(\omega, \underline{\xi}) \sim \frac{i\omega}{8\pi^2 c} \int_S dS \ R \frac{\hat{n} \cdot \hat{r}}{r^2} e^{2i\omega r/c} . \quad (4.62)$$

Here

$$\underline{r} = (x - \xi, y - \eta, z), \quad \hat{r} = \underline{r}/r , \quad (4.63)$$

and, as above,

$$r = \sqrt{(x - \xi)^2 + (y - \eta)^2 + z^2} . \quad (4.64)$$

**Exercise 4.24.** Suppose that the surface  $S$  is cylindrical; that is the surface is defined by a curve in  $x, z$  and lines parallel to the  $y$  axis, so that

$$x = x(\sigma), \quad z = z(\sigma) \quad dS = \sqrt{\gamma} \, d\sigma dy, \quad \gamma = \left[ \frac{dx}{d\sigma} \right]^2 + \left[ \frac{dz}{d\sigma} \right]^2 . \quad (4.65)$$

Carry out the stationary phase in  $y$  in (4.62) to obtain the 2.5-D Kirchhoff approximation. Show that the stationary point is at  $y = \eta$

and

$$u_S(\omega, \underline{\xi}) \sim \frac{\sqrt{|\omega|} e^{3\pi i/4} \operatorname{sgn} \omega}{8\pi^{3/2} \sqrt{c}} \int_C \frac{R e^{2i\omega/c}}{r^{3/2}} \mathbf{n} \cdot \mathbf{r} \sqrt{\gamma} \, d\sigma, \quad (4.66)$$

with  $y = \eta$  in the definition of  $r$ , (4.64).

#### 4.4.3. Verification for a general single surface

In this subsection, we will apply our inversion algorithm in 3-D to an arbitrary single surface. We use the coordinates depicted in Figure 4.1. That is, the generic field point is denoted by

$$\underline{x} = (x, y, z) \quad , \quad (4.67)$$

the generic point on the surface by

$$\underline{x}' = (x', y', z') \quad (4.68)$$

and the generic geophone on the observation surface by

$$\underline{x}_0 = (\xi, \eta, 0) \quad . \quad (4.69)$$

It is further convenient to define vectors relative to the geophones:

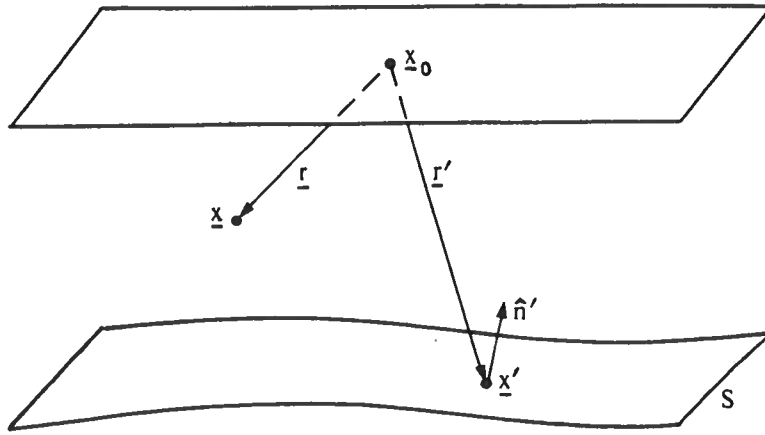


Figure 4.1. Backscatter Reflector Geometry

$$\underline{r} = \underline{x} - \underline{x}_0, \quad r = |\underline{r}|, \quad \hat{r} = \underline{r}/r, \quad (4.70)$$

and

$$\underline{r}' = \underline{x}' - \underline{x}_0, \quad r' = |\underline{r}'|, \quad \hat{r}' = \underline{r}'/r'. \quad (4.71)$$

On inserting the Kirchhoff scattering data from equation (4.62) into the "theory" form of our 3-D algorithm (4.42), and recalling the temporal transform definition,

$$u_S(\omega, \underline{\xi}) \equiv \int_0^\infty dt U_S(t, \underline{\xi}) e^{i\omega t}, \quad (4.72)$$

we obtain

$$\beta(\underline{x}) \sim - \frac{z}{(\pi c)^3} \int d\omega \omega^2 F(\omega) \iint d^2\xi \iint d^2\sigma \sqrt{\gamma} R \frac{\hat{n}' \cdot \hat{r}'}{r r'^2} e^{2i\omega(r' - r)/c}. \quad (4.73)$$

Here we have replaced the generic surface element,  $dS$ , by an explicit parametrization,  $\sigma_1, \sigma_2$ , and have correspondingly introduced the notation,

$\sqrt{\gamma}$ , for the first fundamental form of differential geometry, which is required to express the surface area element in terms of the coordinates,  $\sigma$ :

$$\gamma = \left| \frac{d\underline{x}'}{d\sigma_1} \times \frac{d\underline{x}'}{d\sigma_2} \right|^2 = \left| \det \left[ \frac{d\underline{x}'}{d\sigma_j} \cdot \frac{d\underline{x}'}{d\sigma_k} \right] \right|^2, \quad j,k = 1,2. \quad (4.74)$$

We now wish to do four dimensional stationary phase with respect to the surface parameters and the geophone parameters. To save some writing, we introduce the alternate notations,

$$\begin{aligned} \xi_1 &= \xi, & \xi_2 &= \eta, & x_1 &= x, & x_2 &= y, & x_3 &= z, \\ x'_1 &= x', & x'_2 &= y', & x'_3 &= z'. \end{aligned} \quad (4.75)$$

Before embarking on this somewhat formidable calculation, we pause to once more emphasize the conditions under which the stationary phase calculation is valid. The formal large parameter is proportional to  $\omega$ . However, the actual large parameter must be a dimensionless quantity which measures the other length scales of the problem in terms of the wave length [cf. (3.1)]:

$$\Lambda = \frac{2|\omega|}{c} L = \frac{4\pi f}{c} L \gg 1, \quad (4.76)$$

Here, the conservative choice of  $f$  is some nominal lowest frequency in the observation band -- we recommend taking it as the midpoint of the smooth ramp ascending from zero filter values to unit filter values. The quantity  $L$  represents the generic length scale of the problem and, as mentioned earlier, this restricts the validity of the asymptotics. The candidates for  $L$  are

- (1) The distance from the upper surface to the reflector, say, the average of  $r'$ ;
- (2) similarly, the distance from the upper surface to the output point, the average value of  $r$ ;
- (3) the radii of curvature of the reflector.

In fact, all three of these distances must be many (at least three) wave lengths. It is extremely difficult to see precisely why  $\Lambda$  must be large for these length scales to justify the fourfold stationary phase being carried out here. However, it is possible to draw this conclusion by examining simpler problems, such as the direct Kirchhoff modeling integral computed by stationary phase (2.5-D is even easier!) and the 2.5-D inversion operator.

It is fairly straightforward to explain these requirements on physical grounds. The first is necessary so that the propagation down to the reflector really be wave-like. That is, the response to the point source cannot be identified as being wave-like unless there is sufficient range for the wave structure to occur. Similarly, the output point is a candidate point on the reflector. Thus, the response from that point must also propagate over sufficient range to be identifiable as a wave. Finally, it is only for reflectors "sufficiently flat" on the scale of the wave length that the reflected wave behaves like a slight modification of the reflection of plane waves by plane boundaries. It is the latter type of wave that is predicted by asymptotics.

Thus, without redefining dimensionless variables in (4.72), we use the formal large parameter

$$\Lambda = \frac{2|\omega|}{c} . \tag{4.77}$$

Then, from equation (4.72), the phase to which we will apply the method of stationary phase is

$$\phi = r' - r . \quad (4.78)$$

The first derivatives of our phase function are

$$\frac{\partial \phi}{\partial \sigma_i} = \nabla' r' \cdot \frac{\partial \underline{x}'}{\partial \sigma_i} = \hat{r}' \cdot \underline{t}'_i , \quad i = 1, 2 , \quad (4.79)$$

and

$$\frac{\partial \phi}{\partial \xi_i} = \frac{\xi_i - x'_i}{r'} - \frac{\xi_i - x_i}{r} , \quad i = 1, 2 . \quad (4.80)$$

In the first of these, we have introduced the surface tangents,

$$\underline{t}'_i = d\underline{x}'/d\sigma_i, \quad i = 1, 2.$$

The stationary point(s) is (are) determined by setting these latter derivatives equal to zero. The first pair of conditions yield

$$\hat{r}' \cdot \underline{t}'_i = 0 , \quad i = 1, 2. \quad (4.81)$$

This shows that  $\hat{r}'$  is orthogonal to both surface tangents, i.e., is normal to the surface to within a plus or minus sign. From Figure 4.1 we see that the minus sign should be chosen. Thus,

$$\hat{r}' = - \hat{n}' , \quad (4.82)$$

at the stationary point. This can readily be interpreted to mean that  $\underline{x}'$  is a "specular" ray. This is to be expected: at backscatter the principal contributing ray is normal to the surface. We note that this condition implies that the angle-dependent reflection coefficient reduces to the normal reflection coefficient,

$$R = R_n = \frac{c_1 - c}{c_1 + c} \quad (4.83)$$

where  $c$  is the speed above the reflector and  $c_1$  is the speed below the reflector.

Exercise 4.25. Establish this result.

On setting the second pair of derivatives to zero, we have:

$$\frac{\xi_i - x'_i}{r'} = \frac{\xi_i - x_i}{r}, \quad i = 1, 2 \quad (4.84)$$

On taking the magnitude of this equation, we see that the sine of the angle between  $\underline{x}$  and the vertical is equal to the corresponding sine for  $\underline{x}'$ . Since these angles are confined to the interval,  $(-\pi/2, \pi/2)$ , where the sine function is monotonic, the angles are equal, hence their cosines are equal:

$$\frac{z'}{r'} = \frac{z}{r} \quad (4.85)$$

Combining the last two equations, we can state the stationary point conditions as:

$$\hat{\mathbf{r}}' = \hat{\mathbf{r}} = -\hat{\mathbf{n}}' \quad . \quad (4.86)$$

Thus, at the stationary point,  $\hat{\mathbf{r}}$  and  $\hat{\mathbf{r}}'$  are collinear and in the (anti) normal direction. That is, the main contributions come from field points that lie on the specular, see Figure 4.2.

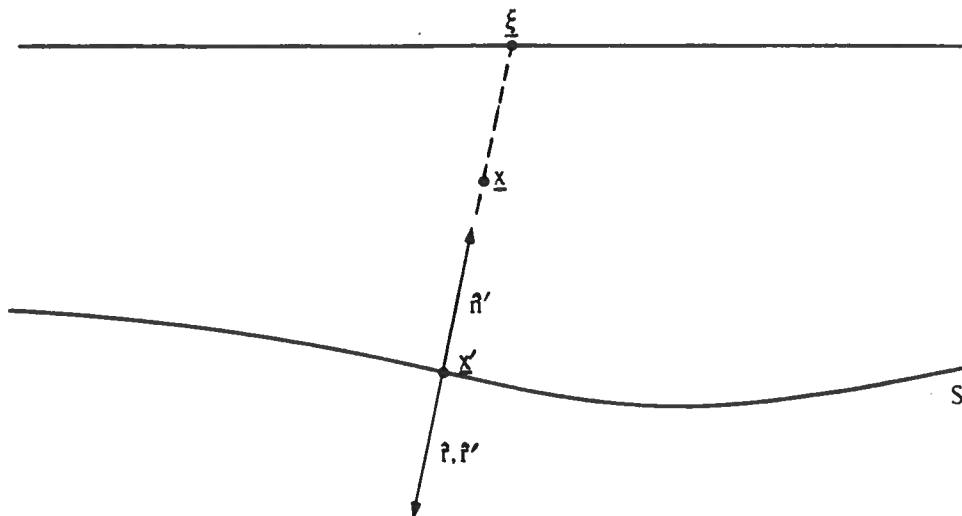


Figure 4.2. Geometry at the Stationary Point

Exercise 4.26. Take magnitudes in the second stationary condition and show that

$$\frac{|\xi - \xi'|}{|\xi - \underline{x}|} = \frac{z'}{z} \quad , \quad (4.87)$$

thus providing a purely algebraic derivation of the collinearity condition.

We can now formally state the stationary phase result as:

$$\beta(\underline{x}) \sim \frac{zR_n}{\pi c} \frac{1}{r r'^2} \sqrt{\frac{\gamma}{|D|}} \int d\omega F(\omega) e^{2i\omega(r - r')/c + i\pi/4 [P \text{sgn}(\omega)]}. \quad (4.88)$$

Here, D and P respectively denote the determinant and signature of the four by four second derivative Hessian matrix of the phase,

$$[\phi_{\xi\sigma}] = \begin{bmatrix} \frac{\partial^2 \phi}{\partial \xi_i \partial \xi_j} & \frac{\partial^2 \phi}{\partial \xi_i \partial \sigma_j} \\ \frac{\partial^2 \phi}{\partial \xi_j \partial \sigma_i} & \frac{\partial^2 \phi}{\partial \sigma_i \partial \sigma_j} \end{bmatrix}, \quad i, j = 1, 2, \quad D = \det[\phi_{\xi\sigma}], \quad P = \text{sig}[\phi_{\xi\sigma}]. \quad (4.89)$$

subject to the stationary phase conditions.

In order to avoid distraction with technical details, we state and postpone the proof of the following

Lemma: For  $\underline{x}$  in a neighborhood of the reflector S,  $P = 0$  at the stationary point.

Now whenever  $P = 0$  at the stationary point, the remaining integral on  $\omega$  yields a band-limited delta function with argument,  $r - r'$ . Moreover, since  $\underline{x}$ ,  $\underline{x}'$  and  $\underline{x}_0$  are collinear at the stationary point, this argument is identical to the normal arclength measured from the reflector -- that is, the singular function of the surface. More precisely,

$$\frac{1}{\pi c} \int d\omega e^{2i\omega(r - r')/c} = \frac{2}{c} \delta(2(r - r')/c) = \delta(r - r') = \delta(s_n), \quad (4.90)$$

where  $s_n$  measures distance normal to the reflector. The fact that  $r - r'$

measures distance normal to S follows from the stationarity conditions. Now we set

$$\delta_B(s_n) = \frac{1}{\pi c} \int d\omega F(\omega) e^{2i\omega(x - r')/c}, \quad (4.91)$$

and rewrite (4.87) as

$$\beta(\underline{x}) \sim \left[ \frac{z}{rr'^2} \right] \sqrt{\frac{\gamma}{|D|}} R_n \delta_B(s_n), \quad (4.92)$$

subject to the stationary conditions.

Thus, under the assumption of the above lemma, we see that the application of our inversion formula to Kirchhoff data does, indeed, yield a scaled singular function of the reflecting surface whenever the stationarity conditions are satisfied. Geometrically, these conditions require that there be some zero-offset point on the data surface for which the normal incidence (specular) ray from that point to the reflector is incident on the reflector at the point being imaged. When there is no such specular ray, the point simply will not be imaged. In terms of our asymptotic analysis, no band limited delta function will be produced for such points on S. This is the effect of limited spatial aperture.

Our asymptotic assumption is that the surface changes gradually. Thus, the neighborhood extends "far from" the reflector (at least three wavelengths). Thus, our conclusion (4.90) holds except (possibly) when P changes value "far away" from the surface. It can be shown that the contributions from such far away "caustics" are negligible, see Armstrong and Bleistein (1978). After the possible changes in sign occurs, P will have one of the values, +2, -2, +4, -4. The results in Cohen and Bleistein

(1983) imply that in the first two cases, the  $\omega$  integral is of asymptotic order,

$$\frac{c}{2\omega|r-r'|} \quad (4.93)$$

But since  $r$  is "far from the surface", this is negligible. Similarly, when  $P$  is  $+4$  or  $-4$ , we obtain a result proportional to a band-limited delta function of  $r - r'$  which is small "far from the surface". Hence, (4.90) holds in a neighborhood of  $S$  large enough that when it no longer holds, the output is negligible compared to its magnitude near  $S$ .

Exercise 4.27. Show that the peak value of  $\delta_B(s_n)$  defined by (4.91) is equal to  $2A/\pi c$ , where  $A$  is the area under the filter in positive  $\omega$ . Suppose instead that the units in frequency domain are Hz, denote by  $f$ , with filter,  $F(f)$ . Then show that the peak value is  $4A/c$ , with units equal to  $(\text{length})^{-1}$ . Reconcile this result with the result of Exercise 4.21.

Since we now know the peak value of the band limited singular function in (4.92), it only remains to determine the peak value of the scale factor. That is, we consider (4.92) when  $\underline{x}$  is on  $S$ . In this case,

$$\underline{r} = \underline{r}' \quad (4.94)$$

and,

$$\underline{x} = \underline{x}' \quad . \quad (4.95)$$

That is, the field point coincides with the specular point -- the main contribution at the geophone  $\underline{x}_0$  comes from the specular (if any) field point(s).

We now evaluate D subject to the stationary conditions and to  $r = r'$ . The second derivatives with respect to the geophone coordinates are:

$$\frac{\partial^2 \phi}{\partial \xi_i \partial \xi_j} = \left[ \frac{1}{r'} - \frac{1}{r} \right] \delta_{ij} - \frac{(\xi_i - x'_i)(\xi_j - x'_j)}{r'^3} + \frac{(\xi_i - x_i)(\xi_j - x_j)}{r^3} \quad , \quad (4.96)$$

$i, j = 1, 2.$

Now use the stationary phase condition (4.83) and further evaluate at  $r = r'$ , since we are doing only the peak value computation. We conclude from (4.54-5) that

$$\frac{\partial^2 \phi}{\partial \xi_i \partial \xi_j} = 0 \quad , \quad i, j = 1, 2. \quad (4.97)$$

Hence, in computing D for  $\underline{x}$  on S, we do not need to evaluate the second partials in  $\sigma$ , since D reduces to the square of the determinant of the mixed partials,

$$D = \left[ \det \frac{\partial^2 \phi}{\partial \sigma_i \partial \xi_j} \right]^2 \quad , \quad i = 1, 2 \quad . \quad (4.98)$$

The mixed partials can be calculated from (4.79) or (4.80):

$$\frac{\partial^2 \phi}{\partial \sigma_i \partial \xi_j} = \frac{1}{r'} \frac{\partial \underline{r}'}{\partial \xi_j} \cdot \underline{t}'_i + \frac{\partial}{\partial \xi_j} \left[ \frac{1}{r'} \right] \underline{r}' \cdot \underline{t}'_{-i}, \quad i = 1, 2. \quad (4.99)$$

The second term vanishes as a consequence of the stationary phase conditions (4.80); thus, making obvious simplifications in the first term, we have

$$\frac{\partial^2 \phi}{\partial \sigma_i \partial \xi_j} = - \frac{1}{r} \frac{\partial \xi}{\partial \xi_j} \cdot \underline{t}'_i, \quad i = 1, 2. \quad (4.100)$$

Letting  $\hat{i}$ ,  $\hat{j}$ ,  $\hat{k}$  denote the standard cartesian unit vectors, we find:

$$D = \frac{1}{r^4} \begin{vmatrix} \hat{i} \cdot \underline{t}'_1 & \hat{j} \cdot \underline{t}'_1 \\ \hat{i} \cdot \underline{t}'_2 & \hat{j} \cdot \underline{t}'_2 \end{vmatrix}^2. \quad (4.101)$$

Using the vector identity,

$$(\underline{a} \times \underline{b}) \cdot (\underline{c} \times \underline{d}) = (\underline{a} \cdot \underline{c})(\underline{b} \cdot \underline{d}) - (\underline{b} \cdot \underline{c})(\underline{a} \cdot \underline{d}), \quad (4.102)$$

we find

$$\begin{aligned}
D &= \frac{1}{r^4} \left[ (\hat{i} \times \hat{j}) \cdot (\underline{t}'_1 \times \underline{t}'_2) \right]^2 \\
&= \frac{1}{r^4} \left[ \hat{k} \cdot \hat{n} \left| \underline{t}'_1 \times \underline{t}'_2 \right| \right]^2 \\
&= \frac{1}{r^4} \left[ \hat{k} \cdot \underline{r} \left| \underline{t}'_1 \times \underline{t}'_2 \right| \right]^2 & (4.103) \\
&= \frac{1}{r^4} \left[ \frac{z}{r} \sqrt{\gamma} \right]^2 \\
&= \frac{z^2}{r^6} \gamma
\end{aligned}$$

Here in the second line we have used the fact that  $\hat{i}$  and  $\hat{j}$  are anti-collinear; in the third line we have used (4.73). Thus, at the stationary point and with  $\underline{x}$  on S (the action point of the band-limited delta function),

$$\sqrt{\frac{\gamma}{|D|}} = \frac{r^3}{z}, \quad \underline{x} \text{ on } S, \tag{4.104}$$

and so the asymptotic evaluation of (4.92) with  $\underline{x}$  on S becomes:

$$\beta(\underline{x}) \sim R_n \delta_B(s_n), \quad \underline{x} \text{ on } S. \tag{4.105}$$

Thus, subject to establishing our lemma, we have completed the verification of our inversion algorithm. Since we know the peak value of  $\delta_B$  on S, we can compute the value of the normal reflection coefficient. Since we know the sound speed above the reflector, we can compute the value below the reflector by using (4.82). This is true for any size of the increment  $\Delta c$  in the sound speed across the reflector.

It remains to establish our lemma.

Lemma: For  $\underline{x}$  in a neighborhood of S,  $P = 0$  at the stationary point.

First observe that for  $\underline{x}$  on S, D is positive by (4.103) as long as the parametrization of the surface by  $\underline{\sigma}$  is well behaved and  $\gamma \neq 0$ . We choose a parametrization for which  $\gamma$  is bounded away from zero for all points on S. However, D is a continuous function of  $\underline{x}$ , defined through its explicit dependence on  $\underline{x}$  plus the conditions of stationarity which make  $\underline{x}'$  and  $\underline{\xi}$  functions of  $\underline{x}$  at the stationary point. Thus, D is different from zero in some neighborhood of S. (In fact, the neighborhood of S where D is nonzero depends on the curvature of the surface S -- i. e., on the principal radii of curvature at each point on S. We choose those to be "many" -- at least three -- wavelengths long. As we have discussed earlier, effects far from the reflector contribute negligibly compared to the peak on the reflector.) When the signature changes value, an eigenvalue of the matrix vanishes. But that, in turn, entails the determinant vanishing. Hence the signature never changes value under the stated conditions -- the signature is a constant at the stationary point in a neighborhood of the reflector S.

We will simplify the computation of this constant by specializing a problem in a manner that will not effect the result. Again, examining (4.103), we see that the eigenvalues do not pass through zero as a function of the principal radii of curvature of the reflecting surface. Thus, we might as well take the reflector to be flat for the purpose of this computation. Furthermore, the eigenvalues will not pass through zero for any choice of  $\hat{n}'$ , so long as this vector does not become horizontal, that is, as long the reflector does not become vertical. Consequently, for the purpose of computing the signature, we might as well take the reflector to

be a horizontal plane. In this case,  $\sigma_1$  and  $\sigma_2$  can be taken to be the cartesian coordinates on the reflector and  $\xi_1$  and  $\xi_2$  can be taken to be the cartesian coordinates on the observation surface. In this case, (4.100) becomes

$$\underline{t}_1 = \hat{i}, \quad \underline{t}_2 = \hat{j}, \quad (4.106)$$

so that the mixed derivative submatrix in the upper left and lower right in (4.89) becomes diagonalized:

$$\frac{\partial^2 \phi}{\partial \sigma_i \partial \xi_j} = \frac{\delta_{ij}}{r}, \quad i, j = 1, 2. \quad (4.107)$$

We already know that the second derivative submatrix in  $\xi$  in (4.89) vanishes at the stationary point when that point is on S, so it only remains to compute the second derivative submatrix in the  $\sigma$ 's:

$$\begin{aligned} \frac{\partial^2 \phi}{\partial \sigma_i \partial \sigma_j} &= \frac{\partial}{\partial \sigma_j} \left[ \frac{\underline{r}'}{r'} \right] \cdot \underline{t}'_2 + \hat{n}' \cdot \frac{\partial^2 \underline{r}'}{\partial \sigma_i \partial \sigma_j} \\ &= \frac{1}{r} \frac{\partial \underline{r}}{\partial \sigma_j} \cdot \underline{t}'_2 + \frac{\partial}{\partial \sigma_j} \left[ \frac{1}{r} \right] \underline{r} \cdot \underline{t}'_2 - \hat{n} \cdot \frac{\partial^2 \underline{r}}{\partial \sigma_i \partial \sigma_j}. \end{aligned} \quad (4.108)$$

Here, in the second line, we have suppressed the primes since  $\underline{x} = \underline{x}'$ . Furthermore, the middle term is zero since  $\underline{r}$  is orthogonal to the surface tangents according to (4.81). To evaluate the first and third term, first note that

$$\frac{\partial \underline{r}}{\partial \sigma_j} = \frac{\partial (\underline{x} - \underline{x}_0)}{\partial \sigma_j} = \frac{\partial \underline{x}}{\partial \sigma_j} = \underline{t}_j , \quad (4.109)$$

so that we obtain

$$\frac{\partial^2 \phi}{\partial \sigma_i \partial \sigma_j} = \frac{1}{r} \underline{t}_i \cdot \underline{t}_j - \underline{n} \cdot \frac{\partial \underline{x}^2}{\partial \sigma_i \partial \sigma_j} \quad (4.110)$$

Our specialized coordinates now play a crucial role in simplifying this set of terms. We use (4.106) to simply the first term. For the second term, we exploit another special feature of our "locally orthogonal arc length coordinate system", namely that the off-diagonal terms are equal to zero and the diagonal terms are  $\pm$  the principle radii of curvature. The choice,  $\pm$ , depends on whether the curve is concave up (+) or concave down (-). In the first case the second derivative and  $\underline{n}$  are collinear, in the second case, they are anti-collinear. We denote those radii of curvature by  $r_1$  and  $r_2$  and we denote the choice of sign ( $\pm 1$ ) by  $\mu_1$  and  $\mu_2$ , respectively. In terms of these variables, we write

$$\frac{\partial^2 \phi}{\partial \sigma_i \partial \sigma_j} = \delta_{ij} \left[ \frac{1}{r} + \frac{\mu_j}{r_j} \right] \quad (4.111)$$

so that the full four by four second derivative matrix is

$$M = \begin{bmatrix} 0 & 0 & -\frac{1}{r} & 0 \\ 0 & 0 & 0 & -\frac{1}{r} \\ -\frac{1}{r} & 0 & \frac{1}{r} + \frac{\mu_1}{r_1} & 0 \\ 0 & -\frac{1}{r} & 0 & \frac{1}{r} + \frac{\mu_2}{r_2} \end{bmatrix} \quad (4.112)$$

Exercise 4.28. Show that

$$\det(M - \lambda I) = \left[ \lambda \left[ \lambda - \frac{1}{r} - \frac{\mu_1}{r_1} \right] - \frac{1}{r^2} \right] \left[ \lambda \left[ \lambda - \frac{1}{r} - \frac{\mu_2}{r_2} \right] - \frac{1}{r^2} \right], \quad (4.113)$$

with roots,

$$\lambda = \frac{1}{2} \left[ \frac{1}{r} + \frac{\mu_j}{r_j} \pm \sqrt{\left[ \frac{1}{r} + \frac{\mu_j}{r_j} \right]^2 + \frac{1}{r^2}} \right], \quad j = 1, 2. \quad (4.114)$$

It can be seen here that two of the roots are always positive (+), and two are always negative (-). Consequently, the signature P of the matrix M is equal to zero, which is what we were to prove. As stated above, by continuity, the signature must be zero in some neighborhood of S, as well.

This result is a special case of the more general result of the following exercise. We will need the generalization in the next chapter.

Exercise 4.29. Establish the following signature lemma: If the symmetric 4x4 matrix M has the form

$$M = \begin{bmatrix} a_1 & 0 & b_1 & 0 \\ 0 & a_2 & 0 & a'_2 \\ b_1 & 0 & a'_1 & 0 \\ 0 & a'_2 & 0 & a'_2 \end{bmatrix} \quad (4.115)$$

then

$$\det M = \begin{bmatrix} \eta^2 - \alpha\epsilon \\ \mu^2 - \beta\delta \end{bmatrix} \quad (4.116)$$

and moreover if each of the factors,  $\eta^2 - \alpha\epsilon$  and  $\mu^2 - \beta\delta$  is positive then

$$\text{sig } M = 0 \quad (4.117)$$

In particular, note that if  $a_1 a'_1 = a_2 a'_2 = 0$  then

$$\det M = \eta^2 \mu^2, \quad \text{sig } M = 0, \quad (a_1 a'_1 = a_2 a'_2 = 0) \quad (4.118)$$

Apply these results to the matrix in equation (4.113) thus giving an alternate proof that its signature is equal to zero.

This completes our analysis of Kirchhoff data. We have seen here that for a single reflector, our inversion formula applied to Kirchhoff approximate data yields a reflector map and an estimate of the sound speed below the reflector in terms of the output and the sound speed above the

reflector. This result did not require small change in sound speed, despite the basis of the inversion in the Born approximation, that is, in small perturbation in sound speed.

On the other hand, in application, if the constant background were not "close" to the "true" propagation speed above the given reflector, then the location would be in error. Furthermore, if the true medium had multiple reflections of significant magnitude from reflectors above the "test" reflector, then the response from the given reflector would be contaminated and the estimate of reflection strength would be inaccurate. Thus, we cannot dispense completely with the small perturbation assumption of the underlying Born-motivated formulation of the inverse problem.

Given these caveats, we might consider using this constant background algorithm locally, applying a "best guess" constant background in different regions. We might also anticipate correcting the background progressively deeper in the earth as more information is generated. This is admittedly more attractive when the theory is no longer limited to a constant. We will see such applications in the Chapter six.

#### 4.5. Implementation and examples

The paper, Bleistein, et. al. (1985), describes the computer implementation of the constant background inversion formulas in 2.5-D and 3-D, including the interpretation of the peak amplitude in the context of the analytical output of the inversions applied to Kirchhoff data. Examples of constant background inversion can be found in Bleistein and Cohen (1982).

We can describe the basic idea of the computer implementation in the context of the formula (4.40). Fast Fourier transform (FFT) is applied to

each trace to transform the data to the frequency domain.

The indicated filter,  $fF(f)$  is applied and the data is inverse transformed, again by FFT, to yield a new data set, say  $W(t, \xi)$  on a uniform temporal grid. In carrying out the sum over geophones, (integral  $d^2\xi$ ), we need  $W(2r/c, \xi)$ . We use three point interpolation in our table of  $W(t, \xi)$  values.

The spatial integration must be computed for each  $\underline{x}$  point for which we seek output. The domain of integration is limited by a number of constraints. In Chapter 3, we discussed these constraints and their implementation. We briefly repeat those ideas here.

The first constraint to be imposed is causality. We cannot integrate over  $\xi$  values for which  $2r/c$  is greater than the maximum time on the trace. It also makes no sense to seek output at points so deep that only one or two traces contribute to this last sum.

The second constraint is spatial aliasing. Let us consider a wave which propagates from the output point  $\underline{x}$  to a surface point  $\xi$ . Associated with this wave is the set of wave numbers in the bandwidth of the data. For each wave number, there is a wave vector whose magnitude is given by the wave number. The transverse component of this wave vector defines a wave which must be sampled at the discrete sample points  $\xi$  of the seismic experiment. This transverse wave vector must be constrained with respect to the transverse sampling rate by an anti-aliasing (Nyquist) condition. For a given wave number, the transverse component of the wave vector increases as the wave travels in directions further inclined to the vertical. Thus, for a bandwidth containing sufficiently high frequencies, this transverse wave vector may have a magnitude which exceeds the spatial Nyquist limit for waves moving more horizontally. Limiting such waves is equivalent to

limiting the spatial domain of integration.

We have seen in the previous section that we image reflectors when there exists a normal incidence ray from the reflector to the domain of the traces on the surface. We can turn that idea around and state that if we know an a priori limit on the angles of inclination of the reflectors in the subsurface, we can limit the domain of integration to include reflectors only up to those angles of inclination.

In practice, we impose all of these constraints.

#### 4.6. Summary

In this chapter we have specialized our integral equation for zero offset constant density wave propagation to the case of constant background sound speed. Under this last assumption, we were able to solve the integral equation in closed form for full bandwidth data. However, seismic data is generally high frequency data for most of the length scales of the earth environment and the propagating frequencies of the seismic experiment. We presented arguments based on Fourier analysis of discontinuous functions to modify our solution in order that the high frequency nature of the data could be exploited to yield a reflector map of the interior of the earth and an estimate of the reflection strength. We then applied this solution to data representing the response to a single reflector. That data was modeled by using the Kirchhoff approximation for the upward scattered wave. By asymptotic analysis, we showed that our inversion formula applied to this data asymptotically yields the reflectivity function of the surface. This function is a scaled singular function. The singular function is a Dirac delta function which peaks on the surface, thereby providing an image of the

reflector. The scale factor turned out to be a known multiple of the normal reflection coefficient when evaluated at the peak value of the band limited singular function. This result provides a means of estimating the sound speed below the reflector in terms of the computed output and the sound speed above the reflector. This determination is not limited to small changes in sound speed, even though the original algorithm was motivated by perturbation theory.

## 5. Towards a High Frequency Inversion Formalism

In this chapter, we will expose the principle ideas behind the development of high frequency inversion algorithms for complex media. All too often mathematical derivations are presented in a manner that completely hides the struggle to produce the results. We will take the opportunity in this chapter to present some of the intellectual history of our education. Since it would not help anyone to follow us down every blind alley we investigated, the development we present here is not an actual temporal history. In fact, although the actual evolution of our ideas largely took place in the context of inversion with a variable stratified medium, we will present our history -- a history of ideas -- in the context of the simpler constant background inversion problem already solved in the last chapter.

As is so often the case in science, at the same time as we were groping our way towards a new formalism for high frequency inversion, a parallel development was going on elsewhere. In early 1985, a brilliant paper by Gregory Beylkin appeared, presenting a powerful view of the inversion problem based on the notions of Radon transforms and pseudo-differential operators. The final approach described here is a blend of the work of Beylkin and his colleagues at Schlumberger (Beylkin, 1984, 1985a, 1985b; Beylkin and Oristaglio, 1985; Beylkin, et al., 1985) and our own (Bleistein 1984, Bleistein and Gray, 1985; Cohen and Hagin 1985; Cohen, et al., 1986; Bleistein, et al., 1985b; Bleistein, 1985, 1986).

### 5.1. Deducing the Inversion Kernel from Kirchhoff Data

The inversion operator (4.42) contains certain features that are common to all such integral inversion operators. Reading that equation from right to left, we see first that each data trace is transformed to the frequency domain, filtered and then transformed back to the time domain, with the temporal evaluation now taking place at  $2r/c$ . We remind the reader that for the upward scattered field represented either by Kirchhoff approximate data, (4.62) or Born approximate data, (4.6), this travel time simply complements the propagation time of the model data, namely,  $2r'/c$ . One may view this as matched filtering, or as adding up data over the diffraction curve associated with a point scatterer at  $\underline{x}$  in a medium with constant propagation speed  $c$ .

With either insight, or with the inversion formula (4.42) as a guide, one might conjecture that the kernel of the inversion operator should always have a phase which is just the travel time from source point  $\underline{x}_s$  to output point  $\underline{x}$  to geophone point,  $\underline{x}_g$ . For our prototype of zero offset, constant background inversion, this does, indeed, reduce to  $2r/c$ .

It only remains, then, to determine the amplitude of the inversion operator. In the previous chapter, we applied our inversion operator to Kirchhoff approximate data and found that the output could be interpreted in terms of the geometrical optics reflection coefficient, which depends nonlinearly on the increment in sound speed across a reflector. We propose now to use that as a criterion for determining the amplitude of the inversion operator. That is, we will require that any inversion operator we set down should produce the singular function of a reflecting surface multiplied by the geometrical optics reflection coefficient of that surface.

We begin by restating the zero offset, constant reference Kirchhoff integral relation (4.62):

$$u_S(\omega, \underline{\xi}) \sim \frac{i\omega}{8\pi^2 c} \int_S \frac{\hat{n} \cdot \hat{r}'}{r'^2} e^{2i\omega r'/c} \sqrt{\gamma} d^2\sigma, \quad dS = \sqrt{\gamma} d^2\sigma, \quad (5.1)$$

with  $\gamma$  defined by (4.74). Here we consider this relation as an integral equation for an unknown reflector  $S$ , with unknown reflection coefficient,  $R$ .

In checking our inversion operator in Chapter 4, we used the method of stationary phase, whose only  $\omega$  dependence was a power of  $|\omega|$  in the combined operation of inversion integral applied to data integral. Thus, we conjecture that the amplitude we seek depends on  $\omega$  only through a multiplicative power. Using the insight that each dimension of stationary phase produces a factor of one over the square root of  $|\omega|$ , we can anticipate the power of  $\omega$  required in the inversion operator. Let us denote the inversion operator by  $W$  and set

$$W[u_S(\omega, \underline{\xi})] = \iint d^2\xi \int d\omega (-i\omega) F(\omega) A(\underline{\xi}; \underline{x}) e^{-2i\omega r/c} u_S(\omega, \underline{\xi}) . \quad (5.2)$$

Here,  $A$  is to be determined. We use (5.1) for  $u_S$  on the right and obtain

$$W[u_S] \sim \frac{1}{8\pi^2 c} \int d\omega \omega^2 F(\omega) \iint d^2\xi \iint_S d^2\sigma R \frac{\hat{n}' \cdot \hat{r}'}{r'^2} \sqrt{\gamma} A(\underline{\xi}, \underline{x}) e^{2i\omega(r' - r)/c} \quad (5.3)$$

Our objective now is to evaluate the integral on the right asymptotically and insist that the result be the reflectivity function  $\beta(\underline{x})$ . Fortunately, for this case, we need do no computations to do this analysis, because the integral is of exactly the same form as (4.73), whose asymptotic analysis

was the main result of Section 4.4.2. However, the asymptotic analysis of (4.73) did, indeed, lead to the result we seek here. That is, if we choose  $A(\underline{x}, \underline{\xi})$  so that the two integrands agree, then  $W[u_S]$  will be  $\beta(\underline{x})$ . Thus, we set

$$A = - \frac{8z}{\pi c^2 r} . \quad (5.4)$$

If we now write out  $W[u_S]$  from (5.2) explicitly with this value of  $A$ , we have a Kirchhoff-based inversion formula:

$$\beta(\underline{x}) \sim \frac{8iz}{\pi c^2} \iint \frac{d^2 \underline{\xi}}{r} \int d\omega \omega F(\omega) e^{-2i\omega r/c} \int_0^\infty dt U_S(t, \underline{\xi}) e^{i\omega t} . \quad (5.5)$$

We see that this result agrees with (4.42), the constant reference, zero offset inversion formula. The Kirchhoff formulation seems to have the advantage of dispensing with the perturbation assumption, but this is only partly true. Indeed, our derivation does not require this assumption for the single surface case treated thus far. But how can we apply the result to the case of a variable sound speed with many layers? The answer is that we must assume that (i) the constant background we choose is "close" to the true background in some sense and (ii) the layers act independently (that is, we must ignore multiples). Any multiples that leak through the preprocessing stage (e.g. stacking) can only be ignored by assuming that they are small. This two assumptions are tantamount to the Born-perturbation assumption in the medium above the reflector being imaged. On the other hand, when these assumptions are satisfied, the estimate of  $R_n$  at the reflector in question is not constrained by a small perturbation assumption. This has been verified in many synthetic tests.

We will not pursue the Kirchhoff integral technique further, but we note that this technique has been successfully applied to the case of pre-stack inversion of common offset gathers in both 2.5 and 3-D, see Sullivan and Cohen (1985). It can also be applied to any of the cases treated by the more general methods to be introduced below.

## 5.2. Deducing the inversion kernel by the asymptotic completeness principle

We now present an inversion principle for the Born integral equation that does not require the use of analytic synthetic data. The reader will note the similarity to the theory of generalized Fourier inversion.

We once more begin from the zero offset Born equation for a constant reference speed, i.e., equation (4.6), with slightly altered notation:

$$u_S(\omega, \underline{x}) = \left[ \frac{\omega}{4\pi c} \right]^2 \iiint d^3 x' \frac{e^{2i\omega x'/c}}{r'^2} a(\underline{x}') \quad , \quad (5.6)$$

Once again we postulate an inversion formula of the form

$$a(\underline{x}) \sim \iint d^2 \xi \, b(\underline{x}, \xi) \int d\omega \, F(\omega) \, e^{-2i\omega x/c} \, u_S(\omega, \xi) \quad , \quad (5.7)$$

where  $b$  denotes an inversion amplitude to be determined. We now note that if this latter formula is correct, then the composite of the last two equations must provide a mapping from  $a(\underline{x}')$  to  $a(\underline{x})$ . Indeed, the composite of these relations has the form

$$a(\underline{x}) \sim \iiint d^3 x' I(\underline{x}, \omega, \underline{\xi}; \underline{x}') a(\underline{x}') \quad (5.8)$$

If this equation is to hold, then of necessity, we must have the following asymptotic completeness relation:

$$I(\underline{x}, \omega, \underline{\xi}, \underline{x}') \sim \delta(\underline{x} - \underline{x}') \quad (5.9)$$

From equations (5.6) and (5.7), we can state the asymptotic completeness relation explicitly for the case of zero offset and constant reference as

$$\frac{1}{(4\pi c)^2} \iint d^2 \xi \frac{b(\underline{x}, \underline{\xi})}{r'^2} \int d\omega \omega^2 F(\omega) e^{2i\omega(r' - r)/c} \sim \delta(\underline{x} - \underline{x}') \quad (5.10)$$

We regard this as an equation for the inversion amplitude  $b$ .

We have written an asymptotic equality and remind the reader that this is a result which is to be true at "high frequency". However, we have integrated over the frequency  $\omega$ . More precisely, we mean that this result is true as long as the range of integration in  $\omega$  [the support of  $F(\omega)$ ] may be viewed as high frequency. As usual, we construct a dimensionless parameter,

$$\Lambda = 2\omega L/c, \quad (5.11)$$

with  $L$  representing the "typical length scales" of the integrand, and require that this parameter be large. Associated with this large parameter is a wave number,  $2|\omega|/c$ . We can think of (5.10) as being required for large values of this wave number. This suggests that we might view (5.10) as an asymptotic equality in the Fourier domain that must be valid for large

values of the magnitude of the transform vector. Indeed, we will adopt that point of view, transform to the wave vector domain, and insist on asymptotic equality there. Introducing the Fourier transform,

$$\hat{f}(\underline{k}) = \iiint f(\underline{x}') e^{-2i\underline{k} \cdot \underline{x}'} d^3x', \quad (5.12)$$

we rewrite (5.10) as an equation in the Fourier domain

$$e^{-2i\underline{k} \cdot \underline{x}} \sim \frac{1}{(4\pi c)^2} \iiint d^3x' e^{-2i\underline{k} \cdot \underline{x}'} \iint d^2\xi \frac{b(\underline{x}, \xi)}{r'^2} \cdot \int d\omega \omega^2 F(\omega) e^{2i\omega(r' - r)/c} . \quad (5.13)$$

We will evaluate the integral on the right for large values of  $k = |\underline{k}|$ . To do so, it will prove convenient to rewrite the integrand in such a manner as to make  $k$  a multiplicative factor of the phase. Thus, we set

$$\underline{k} = k\hat{\Phi}, \quad \omega/c = k\eta \quad (5.14)$$

and rewrite (5.13) as

$$e^{-2i\underline{k} \cdot \underline{x}} \sim \frac{ck^3}{(4\pi)^2} \iiint d^3x' \iint d^2\xi \frac{b(\underline{x}, \xi)}{r'^2} \cdot \int d\eta \eta^2 F(c k \eta) e^{2ik\hat{\Phi}(\underline{x}, \underline{x}', \hat{\Phi}, \xi, \eta)} . \quad (5.15)$$

In this equation, the phase function,  $\hat{\Phi}$ , is defined by

$$\Psi(\underline{x}, \underline{x}', \hat{p}, \xi, \eta) = 2\eta(r' - r) - \hat{p} \cdot \underline{x}' . \quad (5.16)$$

We remind the reader that  $r$  and  $r'$  are as defined by (4.63, 69, 71).

We will apply the method of multidimensional stationary phase to the integral in (5.15), with respect to the six variables  $\eta$ ,  $\xi$ , and  $\underline{x}'$ . The six first derivatives which must be set equal to zero are

$$\frac{\partial \Phi}{\partial \eta} = r' - r , \quad \frac{\partial \Phi}{\partial \xi_i} = \frac{\xi_i - x'_i}{r'} - \frac{\xi_i - x_i}{r} , \quad i = 1, 2 , \quad (5.17)$$

$$\frac{\partial \Phi}{\partial x'_j} = \eta \frac{x'_j - \xi_j}{r'} - \hat{p}_j = \eta r'_j - \hat{p}_j , \quad j = 1, 2, 3 .$$

Here we introduce  $\xi_3 = 0$  to preserve the symmetry of the last equation. Setting the derivatives  $\partial \Phi / \partial x'_j$  equal to zero leads to the conclusion that the unit vectors,  $\hat{r}'$  and  $\hat{p}$ , must be collinear or anti-collinear and that  $\eta$  must have magnitude one; that is,

$$\hat{\eta} r' = \hat{p} , \quad \eta = \pm 1 = \hat{r}' \cdot \hat{p} , \quad \hat{r}' = \pm \hat{p} , \quad (5.18)$$

with the order of plus and minus being the same in both equalities.

Setting  $\partial \Phi / \partial \xi_i$  equal to zero leads to the conclusion that the vector  $\hat{r}$  must be collinear with  $\hat{r}'$ , hence (5.18) is also true when  $\hat{r}'$  is replaced by  $\hat{r}$ . Setting  $\partial \Phi / \partial \eta$  equal to zero leads to the conclusion that  $r = r'$ . However, since  $\underline{r}$  and  $\underline{r}'$  have the same direction and the same initial point, we conclude that at the stationary point

$$\underline{x}' = \underline{x} , r' = r . \quad (5.19)$$

Given a value of  $\underline{x}$  and  $\underline{k}$ , we choose  $\underline{x}'$  as in (5.19) and draw the ray through  $\underline{x}$  with direction given by  $\underline{k}$  (or  $\hat{\underline{p}}$ ). The intersection of this ray with the upper surface determines  $\underline{\xi}$ . Furthermore, we must choose  $|\eta| = 1$ . Thus, in order for there to be a stationary point,  $\underline{k}$  must be in the bandwidth defined by the filter,  $F(\omega)$  and the  $\underline{\xi}$ -domain of integration must contain the direction  $\hat{\underline{r}}$  which is collinear or anti-collinear with  $\hat{\underline{p}}$ . When at least one of these conditions fails, there is no stationary point and the integral is asymptotically lower order in  $|\omega|$  or  $k$ . We proceed under the assumption that there is, indeed, a stationary point, for it is only in such a case that we will require that the asymptotic equality (5.15) hold.

We must now compute the determinant of the 6X6 Hessian matrix of second derivatives with respect to the variables  $\eta, \xi_1, \xi_2, x_1, x_2, x_3$ . This calculation is much like the calculation of the determinant of the 4X4 determinant in Section 4.4.2. We will outline the calculation in a series of exercises.

Exercise 5.1. Denote the Hessian matrix for  $\bar{\Phi}$  evaluated at the stationary point by  $\bar{\Phi}_{ij}$ . Show that  $\bar{\Phi}_{ij}$  has a 3X3 upper left hand corner of zeroes. Hence conclude that  $\det[\bar{\Phi}_{ij}]$  is the square of the determinant of the upper right hand 3X3 matrix whose rows are of the form,

$$\pm \hat{\underline{p}}, (\mp 1/r, 0, 0) \pm f_1 \hat{\underline{p}}, (0, \mp 1/r, 0) \pm f_2 \hat{\underline{p}}.$$

(The actual values of  $f_1$  and  $f_2$  are not important.) Use row elimination to simplify the determinant of the 3X3 matrix and conclude

that

$$\det [\Phi_{ij}] = \frac{p_2^2}{r^4} = \frac{z^2}{r^6} . \quad (5.20)$$

Exercise 5.2. We now proceed to compute the signature of  $\Phi_{ij}$ . First, conclude from (5.20) that  $\Phi_{ij}$  has no zero eigenvalue for any point  $\underline{x}$  in the subsurface; hence, we can determine the signature for a simple special case. Choose the special case for which  $\beta_1 = \beta_2 = 0$ ,  $\beta_3 = 1$  and  $r = 1$ . Show that there are two triple eigenvalues of the form

$$\lambda = [\sqrt{5} \pm 1]/2, [-\sqrt{5} \pm 1]/2,$$

with the choice of ( $\pm$ ) again following the order in (5.18). Since the first expression here is always positive and the second expression is always negative, the same is true of each triple of eigenvalues. Thus,

$$\text{sig} [\Phi_{ij}] = 0. \quad (5.21)$$

We are now prepared to evaluate the integral (5.15) by the method of stationary phase. The result is

$$e^{-2i\mathbf{k}\cdot\mathbf{x}} \sim \frac{\pi c r}{16z} b(\underline{x}, \xi) e^{-2i\mathbf{k}\cdot\mathbf{x}} F(\pm c\mathbf{k}) . \quad (5.22)$$

The filter function  $F$  is a smoothed Fourier transform of an impulse function or one dimensional delta function. Clearly, we can only hope for the right side to be the Fourier transform of a delta function when the function  $F$  is equal to the Fourier transform of a delta function, that is, when  $F = 1$ . In

that case, we can determine the value of  $b(\underline{x}, \underline{\xi})$  by requiring the amplitude on the right to be equal to unity whenever  $F$  is. Thus,

$$b(\underline{x}, \underline{\xi}) = \frac{16z}{\pi c r} . \quad (5.23)$$

and our inversion formula (5.5) becomes

$$a(\underline{x}) \sim \frac{16z}{\pi c} \iint \frac{d^2 \xi}{r} \int d\omega F(\omega) e^{-2i\omega r/c} u_S(\omega, \underline{\xi}) . \quad (5.24)$$

On introducing the factor,  $i\omega/2c$ , we obtain the reflectivity function,

$$\beta(\underline{x}) \sim \frac{8iz}{\pi c^2} \iint \frac{d^2 \xi}{r} \int d\omega \omega F e^{-2i\omega r/c} \int_0^\infty dt U_S(t, \underline{\xi}) e^{i\omega t} . \quad (5.25)$$

which agrees with the result (4.42).

Exercise 5.3. As an alternate to this derivation, proceed by applying the method of stationary phase in  $\underline{\xi}$  directly to (5.10). Obtain an  $\omega$ -integral which can be recognized as a bandlimited one dimensional delta function in  $r' - r$  divided by the square of the same difference. Argue on the basis of distributions in polar coordinates that this one dimensional delta function is, indeed, equivalent to  $\delta(\underline{x}' - \underline{x})$ . This is the approach in Cohen and Hagin (1985).

### 5.3 Toward a Generalization of the Completeness Relation Approach

Having struggled with a six fold stationary phase calculation, we would

be poised to pursue this type of derivation for inversion in more complex cases. However, as indicated earlier, work by Beylkin (1985a) suggests a more elegant solution of the asymptotic completeness relation. Moreover, this approach generalizes at once to cover most of the cases of interest in seismic exploration without requiring as much computation.

We return to the asymptotic completeness relation (5.8):

$$\alpha(\underline{x}) \sim \iiint d^3 \underline{x}' I(\underline{x}, \omega, \underline{\xi}; \underline{x}') \alpha(\underline{x}') \quad . \quad (5.26)$$

Realizing that if this equation has a solution, then the left side must be a delta function, we expand the phase and amplitude about the singular point to obtain

$$r' = |\underline{x} + (\underline{x}' - \underline{x})| = |\underline{x} + (\underline{x}' - \underline{x})| \approx r + r \cdot (\underline{x}' - \underline{x}) \quad . \quad (5.27)$$

and

$$\frac{1}{r'^2} \approx \frac{1}{r^2} \quad . \quad (5.28)$$

On introducing these results into the asymptotic completeness relation we have

$$\iint d^2 \underline{\xi} b(\underline{x}, \underline{\xi}) \int d\omega \omega^2 F(\omega) e^{2i\omega r \cdot (\underline{x}' - \underline{x})} \sim (4\pi cr)^2 \delta(\underline{x} - \underline{x}') \quad . \quad (5.29)$$

Following Beylkin (1985a), we now convert this equation to the form of the classical Fourier completeness theorem by introducing the change of variables,

$$\underline{k} = 2\omega \underline{r}/c \quad . \quad (5.30)$$

Exercise 5.4. Show that the jacobian of this transformation is given by

$$\frac{\partial(k_1, k_2, k_3)}{\partial(\omega, \xi_1, \xi_2)} = \frac{8\omega^2}{c^3} \begin{vmatrix} \frac{\partial \underline{r}}{\partial \xi_1} \\ \frac{\partial \underline{r}}{\partial \xi_2} \end{vmatrix} = \frac{8\omega^2}{c^3} \cdot \frac{z}{r^3} \quad . \quad (5.31)$$

With the result of the previous exercise and the classical result

$$\iiint d^3k e^{ik \cdot (\underline{r} - \underline{r}')} = (2\pi)^3 \delta(\underline{r} - \underline{r}') \quad , \quad (5.32)$$

we readily deduce that the choice

$$b(\underline{r}, \underline{\xi}) = \frac{16z}{\pi c r} \quad (5.33)$$

will satisfy the asymptotic completeness relation. Since this agrees with (5.23), we see that once again we are led to the correct inversion formulas for  $\alpha$  and  $\beta$ .

Exercise 5.5. Obtain the analogous inversion for the 2-D problem (i.e. line sources) by the methods of this subsection.

#### 5.4. Test case: inclusion of field statics

It is now long past time to obtain a new inversion result! As a prelude to a discussion of our recent (1984-1986) papers on this subject, we begin with a modest extension--the accounting for field statics. To incorporate field statics into our inversion, we must allow the observation surface to be curved. We retain our assumptions of zero offset data and a constant reference speed.

The curvatures of the observation surface provides another length scale that must be relatively large in order for our asymptotic methods to apply. Thus, we assume that these curvatures are moderate. In particular, we exclude folds and other violent changes in the topography of the observation surface.

Inversion before (or including) statics has a certain practical appeal, since the static corrections introduce a degree of non-linear amplitude distortion. However, our primary purpose is pedagogical, and we have no intention of claiming to have solved the very difficult statics problem in seismic exploration. For one thing, field statics is the least of the static correction problem -- residual statics correction to compensate for the near surface weathered zone is often much more taxing. To apply our methods to the total statics correction, we would have to assume that the total statics correction gave an equivalent observation datum and that instead of carrying out the statics, we used this surface in the inversion procedure.

Our derivation of the Born integral equation (2.16) admits a curved observation surface. We need merely to allow the source/receiver functions,  $\underline{x}_s$  and  $\underline{x}_g$  to be general functions of the surface parameters,  $\underline{\xi}$ , instead of

just being the cartesian themselves as in the examples we gave in equations (2.23-27).

Again, we expose our ideas in the context of (i) constant reference speed and (ii) zero offset observations. Specializing the Born integral equation (2.16) to this case, we obtain

$$u_S(\omega, \underline{\xi}) = \left[ \frac{\omega}{4\pi c} \right]^2 \iiint d^3 r' \frac{e^{2i\omega r'/c}}{r'^2} a(\underline{x}') \quad (5.34)$$

with

$$r' = | \underline{x}' - \underline{x}_0(\underline{\xi}) | \quad . \quad (5.35)$$

These equations are formally the same as equations (4.6) and (4.7) for the flat datum case, but now  $\underline{x}_0$  is a general function of  $\underline{\xi}$  instead of specifically being  $(\underline{\xi}, 0)$ .

As in the previous section, we postulate an inversion formula of the form

$$a(\underline{x}) \sim \iint_{S_{\underline{\xi}}} d^2 \xi b(\underline{x}, \underline{\xi}) \int d\omega F(\omega) e^{-2i\omega r/c} u_S(\omega, \underline{\xi}) \quad . \quad (5.36)$$

Here,  $S_{\underline{\xi}}$  denotes the range of values in  $\underline{\xi}$  which define the observation surface over which  $\underline{x}_0$  varies. Proceeding as in the previous section by substituting (5.34) on the right side of (5.35) we deduce an asymptotic completeness relation:

$$\frac{1}{(4\pi c)^2} \iint_{S_\xi} d^2\xi \frac{b(\underline{x}, \xi)}{r'^2} \int d\omega \omega^2 F(\omega) e^{2i\omega(r' - r)/c} \sim \delta(\underline{x} - \underline{x}') \quad (5.37)$$

On approximating the phase and amplitude by the power series expansions introduced in the previous section, we deduce the following expression for the inversion amplitude  $b$ :

$$b(\underline{x}, \xi) = \frac{(4\pi c r)^2}{(2\pi)^3 \omega^2} \left| \frac{\partial(k_1, k_2, k_3)}{\partial(\omega, \xi_1, \xi_2)} \right| = \frac{2c^2 r^2}{\pi \omega^2} \left| \frac{\partial(k_1, k_2, k_3)}{\partial(\omega, \xi_1, \xi_2)} \right| \quad (5.38)$$

Thus we see that the formalism of the previous section goes over without change except for the evaluation of the jacobian of Beylkin's transformation.

Exercise 5.6. Introduce the surface tangents

$$\underline{t}_i = \frac{\partial \underline{x}_0}{\partial \xi_i} \quad , \quad i = 1, 2, \quad (5.39)$$

and show that

$$\frac{\partial}{\partial \xi_i} \hat{r} = -\frac{1}{r} \left[ \underline{t}_i - (\hat{r} \cdot \underline{t}_i) \hat{r} \right] \quad , \quad i = 1, 2 \quad (5.40)$$

Exercise 5.7. Use the differential geometry result,

$$\underline{t}_1 \times \underline{t}_2 = \sqrt{\gamma_\xi} \underline{n}_\xi . \quad (5.41)$$

Here,  $\sqrt{\gamma_\xi}$  denotes the differential surface element (defined for the parametrization by  $\xi$  as  $\gamma$  is defined by (4.74) for the parametrization  $\sigma$ ) and  $\underline{n}_\xi$  denotes the downward normal from the observation surface. Show that the transformation jacobian evaluates to

$$\left| \frac{\partial(\underline{k})}{\partial(\omega, \underline{\xi})} \right| = \frac{8\omega^2}{c^3} \sqrt{\gamma_\xi} \frac{\underline{n}_\xi \cdot \hat{r}}{r^2} . \quad (5.42)$$

The previous exercises show that  $b$  is determined as

$$b = \frac{16}{\pi c} \sqrt{\gamma_\xi} \underline{n}_\xi \cdot \hat{r} . \quad (5.43)$$

We note that for a flat datum, the dot product in the previous equation reduces to  $z/r$  and  $\gamma_\xi = 1$ . Hence, we recover the now familiar result of the previous section. The inversion results for the curved datum case are thus

$$\alpha(\underline{x}) \sim \frac{16}{\pi c} \iint d^2\xi \sqrt{\gamma_\xi} \underline{n}_\xi \cdot \hat{r} \int d\omega F(\omega) e^{-2i\omega r/c} \int dt U_S(t, \xi) e^{i\omega t} , \quad (5.44)$$

and

$$\beta(\underline{x}) \sim \frac{8i}{\pi c^2} \iint d^2\xi \sqrt{\gamma_\xi} \underline{n}_\xi \cdot \hat{r} \int d\omega \omega F(\omega) e^{-2i\omega r/c} \int dt U_S(t, \xi) e^{i\omega t} . \quad (5.45)$$

In these formulas, the normal is defined by the parameterization of the

observation datum by equations (5.39) and (5.41).

### 5.5. Generalizations

The lectures will continue with discussions of recent papers. Any of the methods of the last three sections lead to the same inversion algorithm, that is, they produce the same amplitude and phase of the inversion integral.

The theory allows for variable background propagation speed and variable background density, common source, common receiver and common offset between sources and receivers. The simple travel time,  $2r/c$ , is replaced by the geometrical optics travel time and the amplitude involves the geometrical optics amplitude and the generalization of the jacobian, (5.31). The most general formulas simplify somewhat when specialized to 2.5D and/or to  $c(z)$  [and  $\rho(z)$ ] background.

### 5.6. Summary

Via consideration of the simple case of the zero offset constant background sound speed, we have described here three formalisms for determining inversion operators. Each of these three formalisms extends to variable background, sound speed and density variation and to common offset, common source or common receiver experiments. They also allow for a variable upper surface.



## Bibliography

- Abramowitz, M., and I. A. Segun, 1965, Handbook of Mathematical Functions, Dover Publications Inc., New York.
- Ben-Menahem, A., and W. B. Beydoun, 1985, Range of validity of seismic ray and beam methods in general inhomogeneous media - I. General theory, Geophys. J. Roy. Ast. Soc., vol. 82, 207-234. II. A canonical problem Geophys. J. Roy. Ast. Soc., vol. 82, 235-262.
- Beylkin, G., 1984, The inversion problem and applications of the generalized Radon transform, CPAM, vol. 37, pp. 579-599.
- Beylkin, G., 1985a, Imaging of discontinuities in the inverse scattering problem by inversion of a causal generalized Radon transform, J. Math. Phys., vol. 26, no. 1, pp. 99-108.
- Beylkin, G., 1985b, Reconstruction of discontinuities in multidimensional inverse scattering problems: smooth errors vs small errors, Appl. Opt., vol. 24, no. 23, pp. 4086-4088.
- Beylkin, G. and M. L. Oristaglio, 1985, Distorted-wave Born and distorted-wave Rytov approximations, Opt. Comm., vol. 53, no. 4, pp. 213-216.
- Beylkin, G., M. Oristaglio, and D. Miller, 1985, Spatial resolution of migration algorithms, in Acoustical Imaging, ed. A. J. Berkhout, J. Redder, L. F. van der Wal, vol. 14, pp. 155-169, Plenum Press, Amsterdam.
- Bleistein, N., 1984, Mathematical Methods for Wave phenomena, Academic Press Inc, New York, Reviewed in Feb 1985 Geophysics by Beylkin.
- Bleistein, N., 1985, On the imaging of reflectors in the earth, Res. Rep. CWP-038, Center for Wave Phenomena, Colo. Sch. of Mines.
- Bleistein, N., 1986a, Two-and-one-half dimensional in-plane wave propagation, Geophys. Prosp., vol. 34, no. 3, p. to appear, 1986. Center for Wave Phenomena Research Report, CWP-014, 1984.
- Bleistein, N., 1986b, Kirchhoff inversion for reflector imaging and sound speed and density variations, Center for Wave Phenomena Research Report, CWP-041.
- Bleistein, N. and J. K. Cohen, 1979, Direct inversion procedure for Claerbout's equations, Geophysics, vol. 44, no. 6, pp. 1034-1040.
- Bleistein, N. and J. K. Cohen, 1982, The velocity inverse problem - Present status, new directions, Geophysics, vol. 47, no. 11, pp. 1499-1511.
- Bleistein, N., J. K. Cohen, and F. G. Hagin, 1985a, Computational and asymptotic aspects of velocity inversion, Geophysics, vol. 50, no. 8,

- pp. 1253-1265. Center for Wave Phenomena Research Report, CWP-004, 1984.
- Bleistein, N., J. K. Cohen, and F. G. Hagin, 1985b, Two-and-one-half dimensional Born inversion with an arbitrary reference, Res. Rep. CWP-032, Center for Wave Phenomena, Colo. Sch. of Mines.
- Bleistein, N. and S. H. Gray, 1985, An extension of the Born inversion method to a depth dependent reference profile, Geophys. Prosp., vol. 33, pp. 999-1022. Center for Wave Phenomena Research Report, CWP-007, 1984.
- Boyd, W. E. and J. B. Keller, 1986, Inverse elastic scattering in three dimensions, J. Acoust. Soc. Am., vol. 79, no. 2, pp. 215-218.
- Cerveny, V., and F. Hron, 1980, The ray series method and dynamic ray tracing systems for 3-D inhomogeneous media, Bull. Seismol. Soc. Am., vol. 70, 47-77.
- Cerveny, V., I. A. Molotov, and I. Psencik, 1977, Ray Method in Seismology, Univ. Karlova, Praha. Also see Chapter 1, Seismic Shear Waves, Part A: Theory, vol. 15A, Handbook of Geophysical Exploration, K. Helbig and S. Treitel, Eds., Geophysical Press Ltd., London, 1985.
- Cheng, G. and S. Coen, 1984, The relationship between Born inversion and migration for common-midpoint stacked data, Geophysics, vol. 49, no. 12, pp. 2117-2132.
- Claerbout, J. F., 1976, Fundamentals of Geophysical Prospecting, McGraw-Hill Book Co, New York. Reprinted in 1985 by Blackwell Scientific Publications
- Clayton, R. W. and R. H. Stolt, 1981, A Born WKB inversion method for acoustic reflection data, Geophysics, vol. 46, no. 11, pp. 1559-1568.
- Coen, S., 1981, Density and compressibility profiles of a layered acoustic media from precritical incidence data, Geophysics, vol. 68, no. 9, pp. 1244-1246.
- Coen, S., 1982, Velocity and density profiles of a layered acoustic medium from common-source point data, Geophysics, vol. 47, no. 6, pp. 898-905.
- Cohen, J. K. and N. Bleistein, 1977, An inverse method for determining small variations in propagation speed, SIAM J. Appl. Math., vol. 32, pp. 784-799.
- Cohen, J. K. and N. Bleistein, 1979, Velocity inversion procedure for acoustic waves, Geophysics, vol. 44, no. 6, pp. 1077-1085.
- Cohen, J. K. and N. Bleistein, 1979, The singular function of a surface and physical optics inverse scattering, Wave Motion, vol. 1, pp. 153-161.

- Cohen, J. K. and N. Bleistein, 1981, A note on velocity inversion of diffracted waves, Wave Motion, vol. 3, pp. 279-282.
- Cohen, J. K. and N. Bleistein, 1983, The influence of out-of-plane surface properties on unmigrated time sections, Geophysics, vol. 48, no. 2, pp. 125-132.
- Cohen, J. K. and F. G. Hagin, 1984, Velocity inversion using a stratified reference, Geophysics, vol. 50, no. 11, pp. 1689-1700, 1985. Center for Wave Phenomena Research Report, CWP-021.
- Cohen, J. K., F. G. Hagin, and N. Bleistein, 1986, Three dimensional Born inversion with an arbitrary reference, Geophysics, p. to appear. Center for Wave Phenomena Research Report, CWP-031, 1985.
- Craig, M., 1986, The Fourier transform of  $1/r$ , Geophysics, vol. 51, no. 2, pp. 417-418.
- Eiges, R. and S. Raz, 1985, Inversion from finite offset data and the simultaneous reconstruction of the velocity and density profiles, Geophys. Prosp., vol. 33, pp. 339-358.
- Erdelyi, A., W. Magnus, F. Oberhettinger, and F. G. Tricomi, 1953, Higher transcendental functions, McGraw-Hill Book Co, New York.
- Gray, S. H., J. K. Cohen, and N. Bleistein, 1980, Velocity inversion in a stratified medium with separated source and receiver, J. Acoust. Soc. Am., vol. 68, pp. 234-240.
- Hagin, F. G. and J. K. Cohen, 1983, Refinements to the linear velocity inversion theory, Geophysics, vol. 49, no. 2, pp. 112-118. Center for Wave Phenomena Research Report, CWP-003, 1983. See errata in June, 1984 Geophysics.
- Kuo, J. T. and T. F. Dai, 1984, Kirchhoff elastic wave migration for the case of noncoincident source and receiver, Geophysics, vol. 49, no. 8, pp. 1223-1238. See also discussion in May 1985 issue.
- Lahlou, M., J. K. Cohen, and N. Bleistein, 1983, Highly accurate inversion methods for three-dimensional stratified media, SIAM J. Appl. Math., vol. 43, pp. 726-758. Center for Wave Phenomena Research Report, CWP-002, 1983.
- Loewenthal, D., L. Lu, R. Roberson, and J. W. C. Sherwood, 1976, The wave equation applied to migration, Geophys. Prosp., vol. 24, pp. 380-399. Reprinted in SEG reprint series vol. 4: Migration.
- Mager, R. D. and N. Bleistein, 1978, An examination of the limited aperture problem of physical optics inverse scattering, IEEE Trans. Prop., vol. AP-25, pp. 695-699.
- Miller, D., M. Oristaglio, and G. Beylkin, 1984, A new formalism and an old heuristic for seismic migration, in Expanded abstracts of 54th SEG Meeting, pp. 704-707, Soc. Expl. Geophys., Atlanta.

- Miller, D., M. Oristaglio, and G. Beylkin, 1984, A new formalism and an old heuristic for seismic migration, in Expanded abstracts of 54th SEG Meeting, pp. 704-707, Soc. Expl. Geophys., Atlanta.
- Sullivan, M. F. and J. K. Cohen, 1985, Pre-stack Kirchhoff inversion of common offset data, Res. Rep. CWP-027, Center for Wave Phenomena, Colo. Sch. of Mines.
- Raz, S., 1981a, Direct reconstruction of velocity and density profiles from scattered data, Geophysics, vol. 46, no. 6, pp. 832- 836.
- Raz, S., 1981b, Three-dimensional velocity profile inversion from finite-offset scattering data, Geophysics, vol. 46, no. 6, pp. 836-842.
- Schneider, W. A., 1978, Integral formulation for migration in two and three dimensions, Geophysics, vol. 43, no. 1, pp. 49-76. Reprinted in SEG reprint series vol. 4: Migration.
- Schneider, W. A., 1984, The common depth point stack, Proc. IEEE, vol. 72, pp. 1238-1254.
- Schultz, P. S. and J. W. C. Sherwood, 1980, Depth migration before stack, Geophysics, vol. 45, no. 3, pp. 376-393. Reprinted in SEG reprint series vol. 4: Migration.
- Sheriff, R. E., 1980, Nomogram for Fresnel-zone calculation, Geophysics, vol. 45, no. 5, pp. 968-972.
- Stolt, R. H., 1978, Migration by Fourier Transform, Geophysics, vol. 43, no. 1, pp. 23-48. Reprinted in SEG reprint series, vol. 4: Migration and as a Classic Paper of the Past 25 Years in Nov. 1985 issue.